EXPERIMENTALLY SUPPORTED REDUCED ORDER MODELING FOR HYDROKINETIC ENERGY SYSTEM DESIGN

by

Austin Lee Griffin

A Thesis

Submitted in Partial Fulfillment of the

Requirements for the Degree of

Master of Science

Major: Mechanical Engineering

The University of Memphis

May 2024

To my beloved parents,

This thesis represents the culmination of my academic journey, made possible by your support and belief in me. I dedicate this achievement to you both as an expression of my gratitude for the role you have played in my life and continuing education. Thank you for everything.

Acknowledgments

I extend my sincere gratitude to my research advisor, Dr. Yong Hoon Lee, for his invaluable guidance and support throughout my master's studies. His dedication, including many late nights spent assisting and collaborating with me, has been fundamental to my academic and personal growth. I am deeply grateful for his mentorship and the opportunity to work closely together on this innovative research.

Abstract

This research advances the field of hydrokinetic energy by introducing a novel control design approach, termed duct contraction control strategy (DCCS), that dynamically optimizes the power output of ducted horizontal axis hydrokinetic turbines (HAHkT). Focusing on the adjustment of duct contraction ratios (CR) and blade pitch in response to varying flow conditions, this strategy is explored through augmented XFOIL and Blade Element Momentum Theory (BEMT) simulations using QBlade software and experimentation in an open-channel water flume. The study uses a dynamic surrogate model (SM) to predict turbine performance in a wide range of flow regimes, particularly examining how adjustments in CR and blade pitch can maximize energy extraction efficiency. Optimization tests, carried out with a variety of velocity profiles, aim to identify turbine configurations that improve power generation and significantly reduce the levelized cost of energy (LCOE), making hydrokinetic energy a more economically viable option. The findings highlight the potential of precise CR and blade pitch control strategies to improve energy yield and reduce costs, providing a robust framework for the design and operational optimization of hydrokinetic turbine systems. This approach not only deepens the understanding of turbine dynamics, but also contributes to the development of efficient and cost-effective renewable energy solutions.

Keywords: control design, horizontal axis hydrokinetic turbine (HAHkT), duct contraction ratio (CR), blade pitch, XFOIL, Blade Element Momentum Theory (BEMT) surrogate model (SM), optimization, levelized cost of energy (LCOE)

Table of Contents

List of Figures

Chapter 1

Introduction

As global energy demands escalate along with the pressing need for sustainable solutions, this introductory chapter carves out a niche for the exploration of ducted horizontal axis hydrokinetic turbines (HAHkT) and the pioneering Duct Contraction Control Strategy (DCCS). The narrative unfolds the landscape of renewable energy technologies, with a keen focus on the underexplored potential of hydrokinetic energy, setting a backdrop for the ensuing discussion on the motivations behind optimizing these green energy sources. This chapter explores the progress and operational benefits of HAHkT while acknowledging the existing challenges in refining their performance for economic viability. It heralds the research's core objective: to forge a novel control strategy aimed at enhancing turbine efficiency and adaptability, thereby laying a groundwork for the comprehensive investigation detailed in this thesis. Emphasizing the significance of dynamic control systems such as DCCS within the renewable energy spectrum, the introduction foreshadows the methodical journey of this thesis from theoretical innovation to practical validation. It serves as a prelude to a deeper exploration of the realm of hydrokinetic turbines, paving the way for the subsequent sections that delve into the background, aims, objectives, and structural outline of the thesis.

1.1 Background and Motivation

The drive toward sustainable and environmentally benign energy solutions intensifies against the backdrop of soaring global energy demands, propelled by exponential population growth [1, 2]. This urgency is further magnified by the dire environmental consequences of persistent dependence on fossil fuels, a significant contributor to climate change [3]. In this scenario, hydrokinetic energy, derived from the kinetic energy inherent in water bodies, emerges as a promising, yet underexploited, renewable resource [4].

The evolution of hydrokinetic energy conversion technology, from preliminary stages to

full-scale demonstration projects, underscores the potential of this resource, especially in regions with substantial water flows such as rivers and tidal streams [5]. However, the journey towards harnessing hydrokinetic energy efficiently faces numerous challenges, including technological limitations, high initial costs, and the environmental impacts of the deployment of turbines in natural water bodies [4, 6].

Ducted horizontal axis hydrokinetic turbines (HAHkT) stand out for their efficiency and operational advantages, such as lower start speeds and enhanced output capabilities compared to their vertical-axis counterparts [6, 7]. However, optimizing these systems to improve their performance and economic viability remains a significant challenge. Innovations in turbine design, particularly the integration of ducts and advanced control strategies such as the Duct Contraction Control Strategy (DCCS), present a promising path to maximize energy extraction and reduce costs [8].

The DCCS, by dynamically adjusting the duct contraction ratios and the angle of the blade pitch in response to changing flow conditions, represents a novel approach to enhancing the adaptability and efficiency of HAHkT systems [9]. This strategy is explored through a combination of augmented XFOIL and Blade Element Momentum Theory (BEMT) simulations, alongside empirical testing in open-channel water flumes, providing a comprehensive method to predict and improve turbine performance under a wide array of flow conditions [10, 11].

In summary, this section underscores the critical need for innovative solutions such as the DCCS to overcome current limitations in hydrokinetic turbine technology. By enhancing the design and operational optimization of HAHkT, the research aims to pave the way for more efficient and economically viable renewable energy solutions, addressing the pressing global demand for sustainable energy sources.

1.2 Research Aim and Objectives

The primary objective of this thesis is to enhance the design, performance, and control strategies of ducted HAHkT, integral to advancing the sustainable energy paradigm. Amidst

the global urgency for sustainable energy solutions, this research endeavors to unravel the complexities of hydrokinetic energy conversion, aiming to harness its full potential as an environmentally friendly and viable power source. At the core of this pursuit is the innovation of a novel control strategy, the DCCS, which dynamically optimizes the duct contraction ratios and the blade pitch to increase power output dynamically. This strategy addresses the crucial challenges of optimizing performance and reducing energy costs [5].

The foundational research approach was inspired by Bilgen et al. (2022), focusing on a reconfigurable ducted array system [12]. This precedent established a reduced order model emphasizing the ”mechanical” resistance akin to the pressure variation over the flow rate within the duct system. However, the resistance of the rotor was not defined and was left for future determination. This research originally aimed to refine this aspect by adhering to Bilgen's guidelines for duct ratios and optimizing the twist of the rotor blade to improve the power coefficient, thus generating maximum rotor resistance for the specific duct configurations. Empirical data collection, which encompasses amperage, voltage, rotational speed, flow rate, and temperature, facilitated an in-depth analysis, although it was insufficient to definitively determine the exact pressure changes and flow rates across the rotor. Given that ducted turbines are capable of operating efficiently at elevated tip speed ratios (TSR), the blade design was optimized for a TSR of 6, thereby formulating a basis for the DCCS. This control methodology inherently increases the average power generation, surpassing the performance of a traditional straight duct with pitch control, while maintaining the ability to sustain the generator near rated power under varying flow conditions.

The research trajectory was meticulously charted through a mixture of analytical and empirical phases, bridging theoretical innovation with tangible application. The initial stages encompassed XFOIL analyses and BEMT simulations, evaluating the hydrodynamic performance of turbine blades in fluid dynamics contexts. These preliminary studies laid the groundwork for subsequent experimental validations.

Experimentation began with tests on a total convergence nozzle to gauge the turbine's

hydrodynamic response under maximum flow conditions. The insights gained from these initial tests informed subsequent BEMT simulations, which were refined to enhance the understanding of turbine-water interactions. This iterative process led to the conceptualization of a new blade design, optimized for the desired TSR, thus maximizing energy extraction efficiency.

Further empirical endeavors involved the design and testing of three distinct ducts with varying contraction ratios, alongside comprehensive testing of 13 stationary pitch rotor models in these configurations. This rigorous testing regime, which ensures the reliability and repeatability of the data, culminated in the development of a surrogate model (SM). This model effectively simplified the interaction between power output, angular velocity, blade pitch, and water velocity, serving as an invaluable tool for simulating turbine performance under diverse operational conditions.

The research was progressed to execute eight optimization scenarios across four unique velocity profiles, assessing both constrained and unconstrained environments. This phase aimed to examine the effectiveness of the control strategy under varying flow dynamics. The utility of the SM was highlighted by its ability to predict optimal configurations, facilitating enhanced energy extraction. The abilities of the DCCS are further emphasized when compared to the pitch-only control at a constant CR of 1.

This thesis encapsulates the journey from conceptualization to empirical validation, underscoring the innovative evolution of a dynamic control strategy for HAHkT. By amalgamating XFOIL analyses, BEMT simulations, iterative design, and experimental validation, this work not only enriches the academic discourse on hydrokinetic energy conversion but also sets the stage for future research endeavors aimed at translating these theoretical advances into commercially viable and sustainable solutions.

1.3 Thesis Outline

This thesis embarks on an exploratory journey into the realm of ducted HAHkT and the pioneering DCCS. The first chapter sets the foundational stage, unveiling the untapped potential

of hydrokinetic energy, and framing the research's objectives and scope within the urgent context of sustainable energy development.

The second chapter conducts a comprehensive literature review, probing into the existing scholarly discourse on hydrokinetic turbines and their advancements. This review situates the study within the broader spectrum of renewable energy research, pinpointing the innovative niche the DCCS intends to fill and bridging identified research gaps.

In the third chapter, the methodology unfolds in a detailed narrative, starting from hydrodynamic analyses using XFOIL and BEMT within QBlade to refine blade profiles and turbine rotor designs, followed by scale testing in an open-channel water flume across various duct contraction ratios and blade pitches. Post-experimental BEMT simulations confirmed the empirical data, allowing evaluation of the selection of a higher-design TSR. An empirically supported SM was developed, facilitating a design optimization process that examined four distinct water velocity profiles under constrained and unconstrained conditions. This culminated in a focused constraint analysis comparing the DCCS with pitch-only control, underscoring the DCCS's enhanced adaptability and performance optimization. This comprehensive methodological journey from hydrodynamic analysis to empirical testing and optimization encapsulates the systematic and rigorous approach employed to validate the DCCS.

The fourth chapter delves into the results and discussion, offering a critical examination of the experimental design and analysis. It meticulously details the comprehensive testing regimen applied to various rotor models and duct designs, emphasizing the iterative and methodical nature of the experiments. Strategic modifications aimed at optimizing turbine performance are thoroughly evaluated. This chapter highlights the development and empirical validation of the DCCS, showcasing its substantial impact on improving turbine power output and operational efficiency. The narrative methodically dissects the experimental findings, elucidating the enhancements brought about by the DCCS in the context of hydrokinetic turbine optimization.

The conclusion of this thesis underscores the significant advances in renewable energy

facilitated by the DCCS for ducted HAHkT, detailing the dynamic adjustment of duct CR and blade pitch in response to water flow variations to enhance energy extraction. Validated by extensive experimental and QBlade simulation analyses, the DCCS has markedly improved the operational adaptability and reliability of HAHkT systems. This research contributes to improving hydrokinetic energy, optimizing turbine performance, and reducing substantial Levelized Cost of Energy (LCOE), with potential implications for transforming the renewable energy landscape into a more sustainable and flexible domain. Future endeavors will aim to incorporate generator control into DCCS, expand the study to encompass higher-speed flows and larger ducts, and thoroughly evaluate the environmental, regulatory, and economic impacts of the technology. These initiatives seek to extend the study's achievements, advancing the deployment of efficient, scalable, and eco-friendly hydrokinetic energy systems, and thus significantly influencing the diversification and sustainability of global energy resources. The thesis culminates in a detailed exposition, offering a deep dive into its intricate themes and underscoring its significant contributions to renewable energy progress.

Chapter 2

Literature Review

This chapter outlines the progression and technological enhancements of horizontal axis hydrokinetic turbines (HAHkT), from their inception to present-day advanced implementations. It highlights the shift toward sustainable energy solutions and discusses the integration of mechanical engineering and fluid dynamics in turbine design, particularly emphasizing the duct contraction control strategy (DCCS) for optimizing energy output.

The narrative categorizes hydrokinetic systems into turbine and non-turbine types, elaborating on the efficiency benefits of duct augmentation in horizontal axis turbines. It also touches on key technological advancements such as the development of composite blades, structural testing for durability, and the significance of design modifications for improved efficiency.

Furthermore, the hydrodynamic aspects of HAHkT are examined, focusing on optimization of energy extraction and the critical role of blade and duct design in enhancing turbine performance. It also considers the environmental impact and scalability of these systems for practical applications.

Overall, this chapter provides a foundational understanding of HAHkT technology, setting the stage for further exploration of advanced control strategies such as DCCS in the thesis, which aims to improve the efficiency and adaptability of hydrokinetic energy systems.

2.1 Horizontal Axis Turbine History

The evolution of HAHkT is marked by a series of innovations targeting the efficient exploitation of water's kinetic energy. This journey commenced in the 1970s, post-energy crisis, signifying a pivot towards environmentally benign technologies and renewable energy sources [13]. The progression from rudimentary designs to the sophisticated systems available today illustrates the seamless integration of fluid dynamics with mechanical engineering, propelling

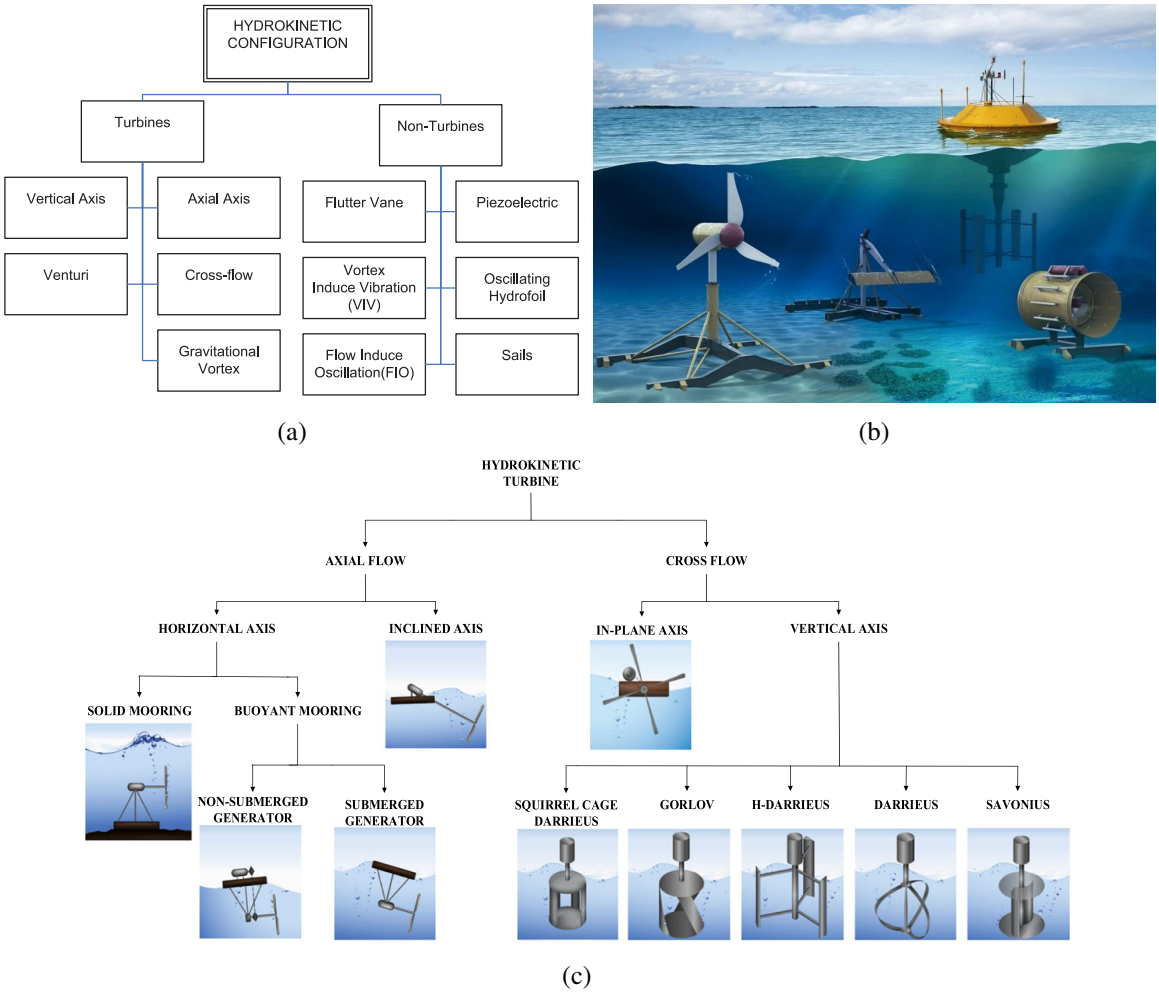

Figure 1: General hydrokinetic options (a) Flowchart of popular hydrokinetic turbine and non-turbine types [14]. (b) Illustration of common hydrokinetic turbine types [15]. (c) Illustration of various axial and cross flow hydrokinetic turbine types [16].

HAHkTs to the forefront of renewable energy advancements.

Hydrokinetic energy systems are divided into turbine and non-turbine categories, each representing unique methods for converting kinetic energy. Figure 1(a) portrays the distinction between these two categories, providing an overview of the hydrokinetic technology spectrum [14]. An in-depth look at hydrokinetic turbines in Figure 1(b) unveils the diversity of turbine types, emphasizing the technological evolution within this realm [15]. The comparison between horizontal and vertical axis turbines, detailed in Figure 1(c), elucidates their operational and

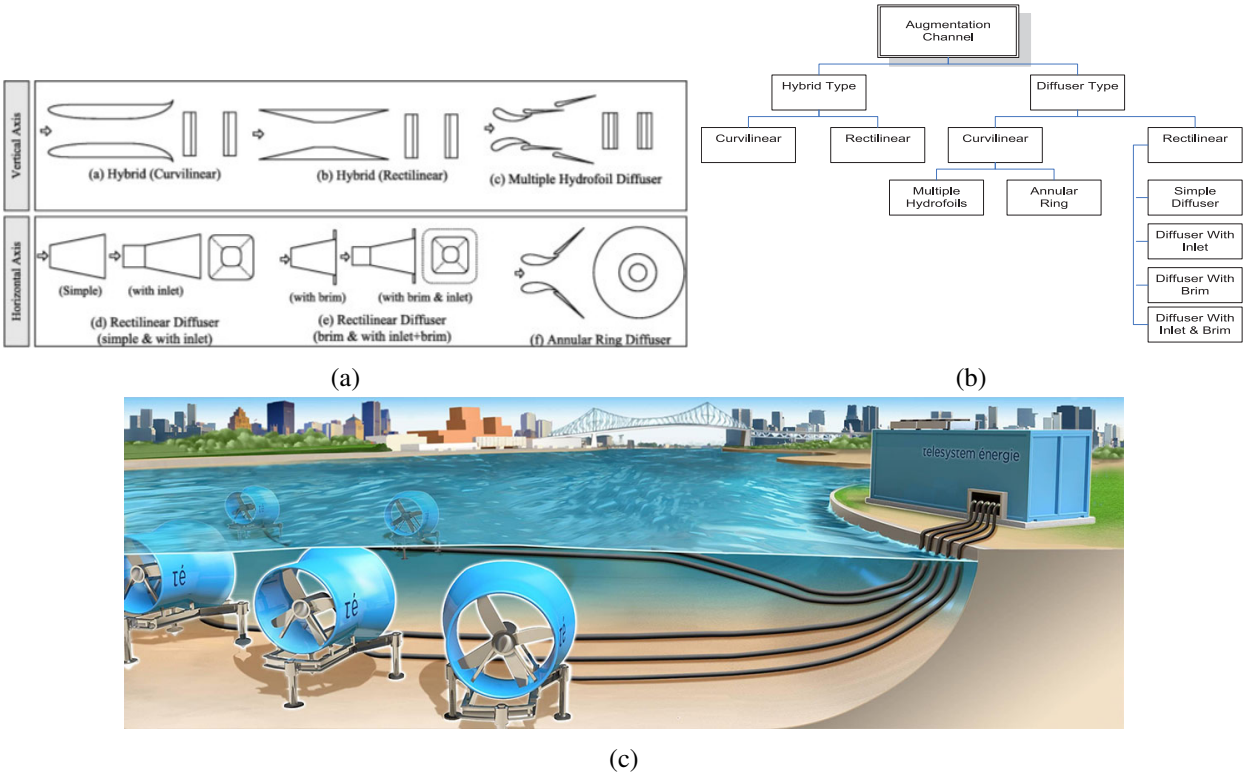

Figure 2: Augmentation Types and a Model of Ducted Hydrokinetic Farm. (a) Various augmentation channels for vertical and horizontal axis hydrokinetic turbine types [17]. (b) Flow chart for various augmentation channels of hydrokinetic turbines [14]. (c) Telesystem énergie's model of a ducted hydrokinetic farm in a river [18].

design differences, with horizontal axis turbines noted for their superior efficiency and consistent power output [19].

The role of augmentation channels or ducts is critical in enhancing the performance of HAHkTs. These mechanisms, designed to streamline the flow of water towards the turbine blades, significantly increase the efficiency of the system [7]. Wang et al. (2012) elucidate the benefits of employing ducts, such as downstream pressure reduction, energy flow concentration, and mitigation of tip losses, thus increasing extracted power [20]. Figure 2(a) visualizes the various duct configurations for both vertical and horizontal axis turbines, showcasing the potential for improved efficiency and environmental harmony. Furthermore, Figure 2(b) presents a detailed classification of these duct designs, from hybrid and diffuser types to curvilinear and

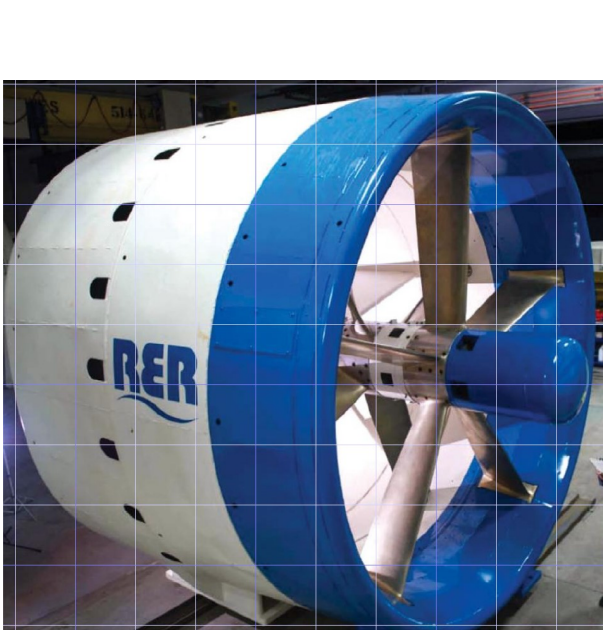

(a)

(b)

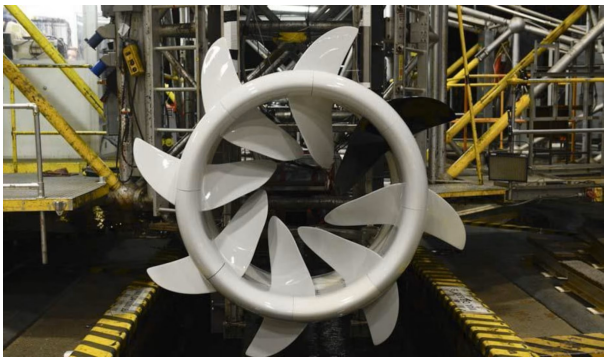

(c)

Figure 3: Recent ducted hydrokinetic projects: (a) RER Hydro Trek: tidal 340 kW ducted hydrokinetic turbine [21], (b) OpenHydro: 300 kW open-center tidal ducted hydrokinetic turbine [22], (c) Oceana Energy Company: open-center 8.15 kW hydrokinetic turbine [23].

rectilinear forms, offering numerous options for energy optimization [14].

Figure 2(c) illustrates Telesystem énergie's model of a ducted hydrokinetic farm in a river environment, demonstrating the practical application of duct integration to enhance the energy capture of flowing waters [18].

Recent advancements in ducted HAHkT technology are underscored in Figure 3, with projects by RERHydro, OpenHydro, and Oceana exemplifying the transition from theoretical models to practical applications. These projects, detailed in Figures 3(a), 3(b), and 3(c), highlight the power density and operational efficiency of hydrokinetic turbines, aligning them with the performance metrics of wind turbines at certain flow velocities [24]. However, the commercial adoption of these turbines, especially the ducted variants, is often hampered by economic and technical misconceptions, especially in challenging environmental settings [25].

The deployment of the RER Hydro TREK system in the St. Lawrence River, together with the initiatives by OpenHydro and Oceana, reflects the practical progress and burgeoning feasibility of hydrokinetic systems. These projects validate the effectiveness of axial flow turbines, akin to those used in wind energy, for marine environments at the megawatt scale, heralding a new era in hydrokinetic technology [10].

This account, enriched with visual aids and detailed categorizations, not only maps the evolution of HAHkT technology but also establishes a basis for ongoing innovation. It emphasizes the critical role of novel design and control methodologies in optimizing turbine performance and energy extraction, setting the stage for future developments in advanced control strategies, including the duct contraction control strategy (DCCS), to enhance the adaptability and efficiency of hydrokinetic energy systems [5, 21, 26].

2.2 Technological Highlights

This section explores the significant technological advances in hydrokinetic turbines, with a focus on the design and control strategy enhancements that are central to this thesis. These innovations are pivotal in the advancement of hydrokinetic energy as a sustainable and efficient solution, aligning with the DCCS introduced in this research.

Integration of advanced hydrokinetic systems into commercial settings signifies a key shift towards more effective use of water flows. The emphasis on diverse configurations such as axial, cross-flow, and oscillating turbines indicates a versatile and adaptable approach to energy capture, reflecting the industry's readiness to harness water currents in various environments [5].

A significant advancement in turbine blade technology is the development of fiber-reinforced composite blades for 1 MW tidal turbines, marking substantial progress in materials science and manufacturing techniques. These innovations bolster the performance and reliability of turbines, ensuring their long-term efficiency and durability, particularly in harsh marine conditions [27]. Rigorous structural testing, encompassing both static and fatigue evaluations, is crucial to validate the design and quality of tidal turbine blades. Such testing

confirms their ability to withstand the stresses of marine environments and their suitability for prolonged operation [27].

Design enhancements aimed at increasing the overall efficiency of ducted turbine systems, such as modifying blade pitch and twist, significantly affect the energy extraction capabilities of these systems [28]. Optimizing chord length and pitch angle is essential to attain high lift coefficients, especially at elevated relative velocities, crucial for turbine hydrodynamic performance [29]. The concept of Control Co-Design, where blade pitch and generator controllers are designed concurrently with the turbine, yields an optimized system [30, 31]. Implementing individual blade pitch control, as opposed to collective adjustment, reduces power fluctuations, increases rolling velocity, and decreases pitching rate [32].

Predictive maintenance technologies and predictive hydrodynamic models are essential to improve turbine management and design. These technologies aim to prevent failures, reduce maintenance costs, and assist in designing and optimizing turbines based on tidal, river, and wind circulations [5, 26].

The challenges of hydrokinetic energy conversion necessitate focused research on site evaluation, turbine design for optimal performance, wake modeling, and environmental impact assessments. Figure 4 exemplifies a wake model critical for reducing wake and planning turbine farms [5].

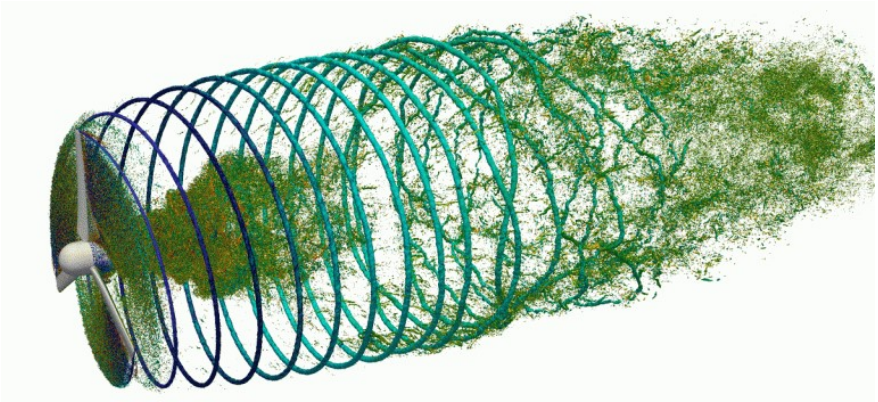

Figure 4: Rotor Wake Simulation Example [33]

Innovative solutions for blade design, such as optimization techniques to mitigate cavitation, address technical challenges in hydrokinetic energy conversion. The potential for large-scale HAHkT applications highlights the continuous need for advancements in technology and control strategies to improve energy extraction [26, 34]. The adaptability and modularity of hydrokinetic technologies, facilitated by the optimization of diffusers and blades, expand the scope for the capture of renewable energy from water flows, underlining the viability of hydrokinetic systems as a sustainable energy source.

The technological advancements detailed in this section not only resonate with the theme of this thesis but also reflect the ongoing progress in the hydrokinetic energy sector. Integration of advanced materials, structural testing, predictive maintenance, and design optimization are making hydrokinetic turbines a more sustainable and efficient renewable energy source. These developments lay a solid foundation for further exploration of control strategies, such as DCCS, aimed at improving the adaptability and efficiency of hydrokinetic energy systems, directly supporting the goals of this thesis.

2.3 HAHkT Hydrodynamics

The exploration of hydrodynamics in ducted HAHkT offers significant insight into the advancements of renewable energy technology. This exploration is highlighted by the innovative DCCS, which aims to optimize energy extraction efficiency through the intricate interplay of fluid mechanics and turbine design.

2.3.1 Flow Characteristics Around a Turbine

Understanding the flow dynamics around turbines is pivotal, as it underscores the potential of ocean currents for robust energy extraction, attributed to the high density of water [10]. Analyzing downstream velocity profiles is essential for the optimization of turbine arrays, stressing the importance of flow dynamics in turbine design and layout [35]. The incorporation of a duct can substantially enhance the flow rate through the turbine rotor, influencing efficiency

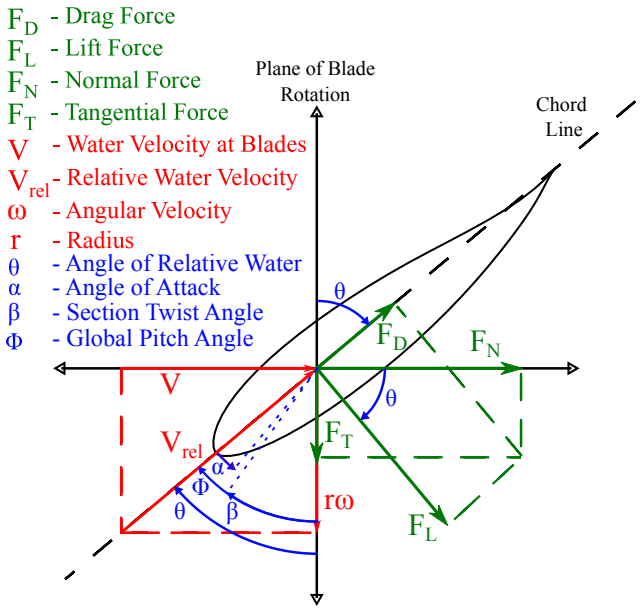

Figure 5: Hydrodynamic forces on the blade profile [38]

and energy capture, while variable speed rotors are known to offer improved efficiency over their fixed-speed counterparts [8, 24].

2.3.2 Hydrodynamic Forces on Blades

Optimization of hydrodynamic forces on the blades requires a thorough examination of the lift and drag coefficients, with the aim of maximizing lift while minimizing drag, with special consideration of the challenges posed by cavitation [36]. Cavitation, a phenomenon in which the local fluid pressure drops below its vapor pressure causing vapor bubbles, is a significant factor in the selection of hydrofoils for hydrokinetic turbines [37]. Optimizing hydrofoil design to mitigate the adverse effects of cavitation is crucial, as thinner hydrofoils generally offer higher lift-to-drag ratios but require robust structural designs to withstand the physical stresses encountered by large turbines [34].

Figure 5 illustrates the forces at play on a hydrofoil [38]. Yunus (2010) notes that the drag and lift coefficients are proportional to the respective forces and inversely proportional to the density of the fluid and the flow velocity [39]. The distinction between pressure drag and

skin drag is vital, with the former influenced by body shape and reducible through design, and the latter arising from fluid viscosity and surface shear stress. This understanding is crucial for an effective hydrofoil design, especially in mitigating cavitation and optimizing hydrodynamic performance.

Identifying the angles of stall, where the blade ceases to generate lift, is a key design consideration. Tools such as XFOIL are essential for plotting the relationships between lift, drag, and angle of attack, providing valuable data on hydrodynamic performance and hydrofoil design constraints [40].

2.3.3 Impact of Blade and Duct Design

Recent advances in blade design and materials have significantly influenced the efficiency of tidal turbines [27]. The hydrodynamic efficiency is greatly affected by the blade design, with optimal configurations that improve energy conversion [41]. Appropriate hydrofoil profiles have been identified for hydrokinetic applications due to their favorable performance characteristics [37, 42]. Moreover, designs that incorporate variable chord and twist not only improve the structural performance of the turbine, but also maintain hydrodynamic efficiency [11].

The power output of a turbine is directly proportional to the cubic power of the flow velocity, underscoring the need to optimize flow to enhance energy capture [24]. Duct augmentation, exploiting the Venturi effect to increase velocity within contraction, is crucial to maximize energy capture [4, 43]. Ducted designs, especially those equipped with self-balancing features, are well suited for deployment in challenging marine environments, where efficiency can be significantly influenced by water dynamics [44]. Ducted turbines, compared to their unducted counterparts, not only perform better in terms of power generation, but also contribute to substantial CO_2 savings, with controlled diffusion at the turbine outlet that could increase the power output by more than 30% [13, 25, 45].

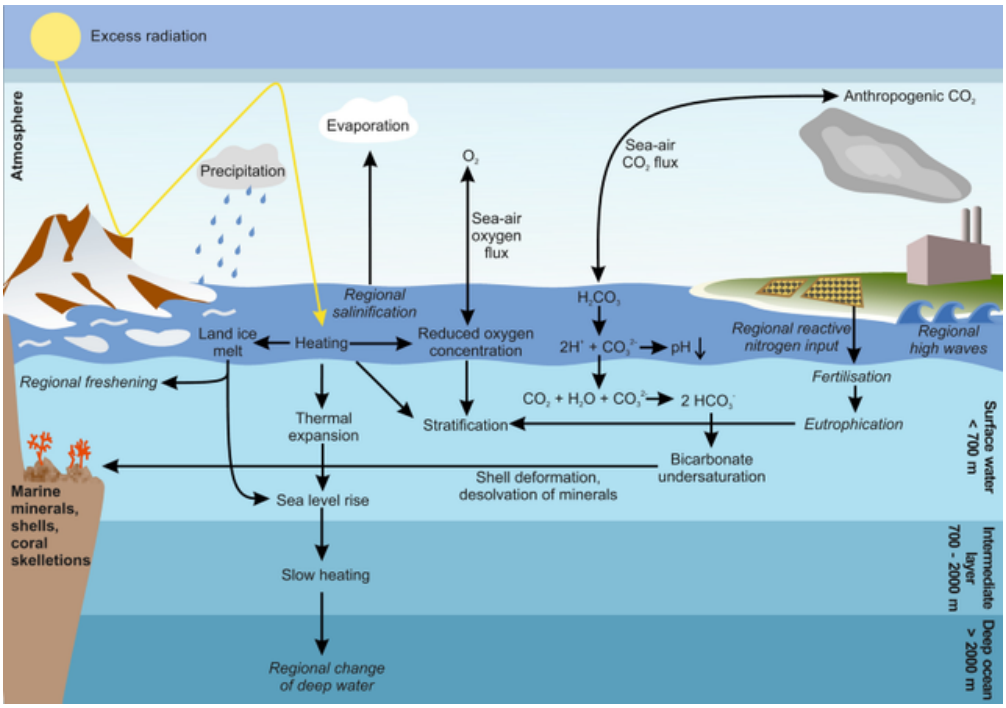

Figure 6: Oceanic Water Cycle [49]

2.3.4 Scalability, Environmental, and Other Considerations

Transitioning hydrokinetic turbines from laboratory prototypes to scalable, real-world applications requires adhering to scaling laws that utilize dimensionless parameters, which are crucial for accurately extrapolating small-scale model data to full-scale turbine prototypes [46, 47]. In addition, environmental considerations play an important role in the selection of locations for turbine installation. Factors such as noise, vibrations, and structural impacts on sediment and hydrological regimes, along with potential disruptions to marine industries such as fishing and shipping, must be carefully evaluated [48]. Ideal site selection should minimize ecological disturbances while harnessing strong and stable flow, taking into account factors such as depth, proximity to the shore, and favorable topography for energy extraction [10].

Furthermore, the deployment of large-scale turbine arrays requires a comprehensive assessment of potential ecological impacts, ensuring that the benefits of renewable energy are not overshadowed by significant environmental trade-offs [5]. Hydrokinetic systems, especially those

integrated into existing water infrastructures, offer a pragmatic approach to enhance renewable energy capacities with minimal additional environmental impact, underscoring the compatibility of hydrokinetic energy with aquatic ecosystems [6].

These systems must also withstand the harsh corrosive conditions of marine environments, possibly requiring the use of sealant, paint, galvanization, and specially designed corrosion-resistant materials [50]. The water cycle, as illustrated in Figure 6, introduces unique challenges to turbine efficiency, such as thermal stratification, where layers of water at different temperatures can significantly influence density and flow characteristics, thus affecting turbine performance at various locations and depths in the ocean [51].

In conclusion, the design, optimization, and implementation of advanced control mechanisms are critical for the development of durable, efficient, and adaptable hydrokinetic turbines. These elements, coupled with a thorough understanding of the net costs that encompass capital, mooring, maintenance, and operational expenses, underscore the multifaceted nature of hydrokinetic energy deployment [24].

Chapter 3

Methodology

This study presents a detailed methodology designed to optimize the performance of ducted horizontal axis hydrokinetic turbines (HAHkT) through an integrated approach. Initially, the design goal for the HAHkT system is established, focusing on the maximization of power achieved through the implementation of a Duct Contraction Control Strategy (DCCS) and adjustments in blade pitch. The methodology advances with comprehensive simulations using QBlade software, where XFOIL analysis is employed to refine the hydrodynamic profile of the blades and Blade Element Momentum Theory (BEMT) is applied to evaluate the overall turbine performance.

The experimental phase is meticulously planned, encompassing the design and assembly of the testing apparatus, which facilitates the acquisition of critical data such as power, flow rate, temperature, and rotational speed. The data collected serve as the basis for constructing a surrogate model, which dynamically captures the performance characteristics of the HAHkT system. Utilizing this model, a surrogate-based optimization process is undertaken, examining various velocity profiles to fine-tune the pitch control and DCCS mechanisms.

The impact of DCCS is thoroughly assessed through comparative analyses between the combined effects of DCCS and pitch control against the scenario where only pitch control is implemented. This comprehensive evaluation helps to substantiate the efficacy of DCCS in enhancing the turbine's operational performance. The complete methodology depicted in Figure 7 illustrates the systematic and iterative nature of the process, ensuring robust and efficient optimization of the HAHkT system.

This approach, which combines theoretical simulations with empirical data and advanced modeling techniques, outlines a coherent and structured pathway to achieving optimized turbine performance, addressing the complex dynamics of fluid-structure interactions in hydrokinetic energy conversion systems.

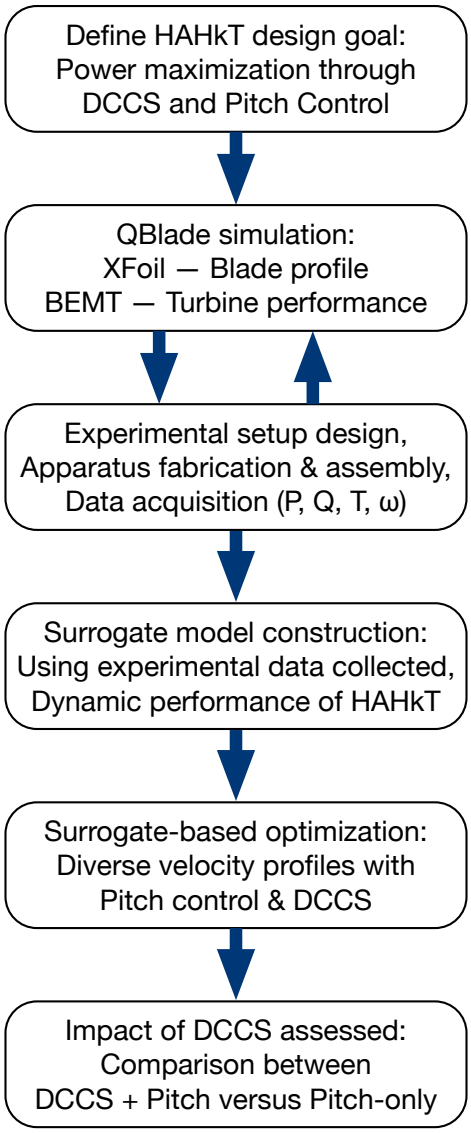

Figure 7: Comprehensive Methodology Flowchart for HAHkT Performance Optimization

3.1 Numerical Methods and Modeling

QBlade, a comprehensive simulation software developed by TU Berlin, is adept at performing BEMT simulations to meticulously analyze turbine blades, incorporating specific hydrofoil geometries across distinct radial sections of the blade [52, 53]. Originally conceived for wind turbines, QBlade has proven its versatility by extending its functionality to the design of HAHkT, leveraging its capabilities in aerodynamic and aeroelastic simulations [10]. For the

design, development and optimization of hydrokinetic turbines, it is valid to apply the same aerodynamic principles as those used by wind turbines [43]. A distinguishing feature of QBlade is its user-friendly interface, which simplifies the pre-simulation process by necessitating the execution of critical tasks such as XFOIL analyses and their subsequent $360°$ extrapolation for precise hydrofoil geometry and Reynolds number assessments [52]. These features make QBlade an indispensable tool in the numerical modeling of hydrokinetic turbines, providing the computational support necessary for XFOIL and BEMT simulations.

3.1.1 XFOIL Analysis

The integration of XFOIL into QBlade software improves hydrodynamic force analysis, providing detailed information on lift coefficients (C_L) and drag coefficients (C_D), as well as moment coefficients, in a wide range of angle of attack. This analytical method, tailored for specific hydrofoil geometries and Reynolds numbers, is crucial in determining the most advantageous initial angle of attack for blade design. This angle is essential to optimize the performance of hydrokinetic turbines by maximizing energy extraction efficiency [53, 54]. To complement the XFOIL analysis, QBlade applies the Viterna method to extrapolate hydrodynamic data over a complete $360°$ span of attack angles. This extrapolation, performed in various sections along the blade, from the root to the tip, according to distinct Reynolds numbers, results in an exhaustive polar data set. This data set is invaluable for further simulations, offering a nuanced understanding of blade performance throughout its entire operational range.

XFOIL's utility extends beyond mere data generation; it is acclaimed for its precision in hydrofoil optimization, particularly at subcritical Reynolds numbers. This specificity makes it an indispensable tool in the design of hydrofoils that maintain high performance under a variety of fluid dynamic conditions [55]. Furthermore, XFOIL facilitates the identification of stall angles across different hydrofoil profiles by plotting C_D and C_L, along with their ratios, against the angle of attack. This capability is critical because the angle of stall delimits the limit beyond which the hydrofoil ceases to generate lift efficiently, which adversely affects the performance of

the turbine. Understanding the stall behavior of hydrofoils through XFOIL analysis helps refine the blade design to avoid adverse hydrodynamic stall effects, thus ensuring consistent and reliable turbine operation [40].

Incorporating XFOIL into the design process through QBlade not only enriches the depth of hydrodynamic analysis but also streamlines the optimization of hydrokinetic turbines. By meticulously evaluating and extrapolating hydrodynamic characteristics, HAHkT designers can make informed decisions about blade geometry, significantly impacting turbine efficiency and longevity.

3.1.2 Momentum Theory

The Momentum Theory, which utilizes the Actuator Disc Model, provides an essential framework for analyzing the operation of HAHkT. This theory simplifies the turbine to an actuator disc that exerts a thrust on the fluid, inducing a change in momentum that is fundamental for the extraction of energy from fluid flows [56, 57]. Under the assumptions of a steady, incompressible and axisymmetric inflow of an inviscid ideal fluid, actuator disc theory may be applied [58]. By applying the principles of mass and momentum conservation, it offers equations to approximate the turbine's energy-harvesting efficiency, introducing the Betz limit. This principle delineates that a turbine can convert no more than 59.3% of the kinetic energy of a fluid, setting an upper efficiency limit [10, 59, 60].

Despite its idealized assumptions, momentum theory is instrumental in understanding how the characteristics of fluid flow and turbine geometry impact energy capture [7]. It sets a foundational benchmark for evaluating turbine performance and encourages further exploration into more detailed models for a comprehensive analysis.

Figures 8(a) and 8(b) illustrate the rotating annular stream tube notation and the evolution of one-dimensional momentum, velocity, and pressure in the flow, respectively. These figures highlight the conceptual underpinnings of the Momentum Theory, visually elucidating the theory's core principles.

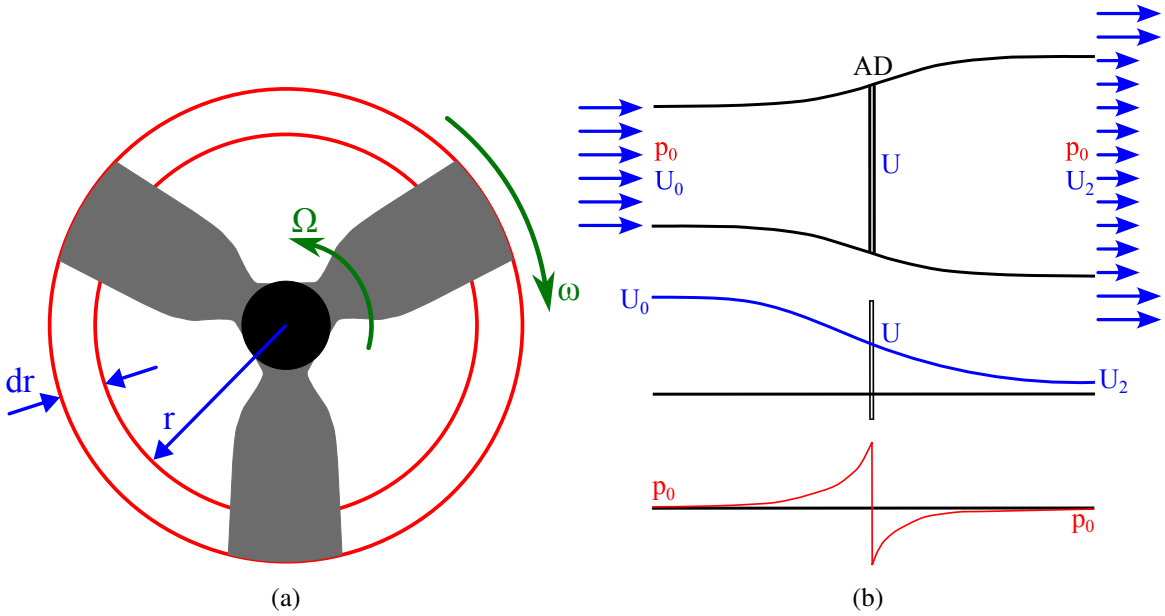

Figure 8: Momentum Theory (a) Rotating annular stream tube notation [61] (b) One-dimensional theory with velocity and pressure evolution [58]

The Actuator Disc Model, a cornerstone of Momentum Theory, streamlines the performance analysis of turbines by focusing on estimations of power output and rotor thrust, absent detailed turbine design specifics. This model is vital to laying the groundwork for more comprehensive analytical models, facilitating an initial assessment of turbine performance that precedes the application of more sophisticated theories. This approach is essential for developing a foundational understanding of turbine efficiency and design optimization, as supported by the recognition of its importance in turbine performance analysis [41].

3.1.3 Blade Element Theory

Blade Element Theory (BET) is a fundamental approach in the hydrodynamic analysis of turbine blades, segmenting the blade into discrete elements for a detailed evaluation of hydrodynamic forces [62, 63]. It combines hydrodynamic principles, particularly lift and drag, to evaluate the forces exerted on each segment, significantly influencing the turbine's torque and power output. It makes the assumption that the flow at any given radius is two-dimensional

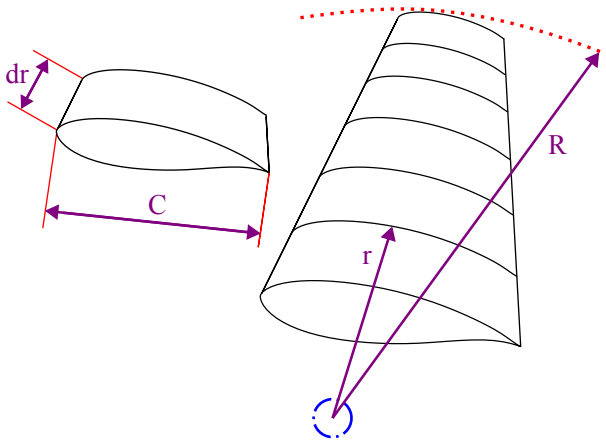

Figure 9: Blade Element Model [61]

and that the hydrofoil behavior is isolated [7, 64]. The detailed methodology of BET provides a deeper understanding of how modifications in blade geometry, blade pitch angle, and operational environments affect turbine efficiency. It acknowledges the variation in flow across the blade's span, allowing for a comprehensive understanding of blade-to-fluid dynamics. This theory is crucial in refining blade designs to ensure optimal performance under varying conditions. By examining each blade element, BET assists designers in adjusting blade characteristics such as pitch distribution and twist to enhance energy extraction efficiency. Figure 9 depicts the blade element model, underscoring the BET's capacity for precise hydrodynamic modeling section by section.

Moreover, BET's application in designing and analyzing the performance of hydrokinetic turbines has shown alignment with empirical data, affirming its effectiveness in refining blade configurations for optimal performance. The theory facilitates the precise adjustment of the lengths of the blade chords and the twist angles, crucial to maximizing the lift coefficients and ensuring efficient operation across a range of velocities, thus highlighting its relevance in hydrodynamic optimization [34].

Despite its comprehensive analysis potential, BET has limitations, particularly in addressing complex three-dimensional flow effects [62]. These challenges highlight the need

to integrate BET with other modeling techniques to capture the full scope of blade dynamics. However, BET remains an indispensable tool in the turbine blade design toolkit, providing a solid foundation for the development of turbines that deliver high efficiency in diverse flow conditions.

3.1.4 Blade Element Momentum Theory

Blade Element Momentum Theory (BEMT) represents a harmonious integration of Momentum Theory and Blade Element Theory principles, establishing a comprehensive analytical framework for turbine performance analysis. This synergy enables the detailed examination of fluid momentum changes and hydrodynamic forces on individual blade elements, facilitating significant advancements in blade design, pitch control, and turbine structuring for optimized energy extraction from fluid flows [41, 53]. BEMT's distinctive ability to accurately model the interaction between blade design elements and surrounding flow conditions has proven instrumental in achieving notable improvements in turbine efficiency. Although QBlade is unable to accept duct inputs, it is still essential to perform BEMT simulations with the rotor experiencing the augmented speeds expected from a convergent duct.

Intricately combining the essence of the two previously mentioned theories, BEMT operates on a steady, two-dimensional basis, drawing from the equivalence between the circulation and momentum theories of lift. This approach allows for an accurate estimation of the inflow distribution along the blade span, which is crucial to identify the optimal geometry of the hydrokinetic turbine blade. By dividing the turbine blade into numerous elementary stream tubes radially, BEMT applies a detailed force balance involving two-dimensional profile lift and drag, as well as the thrust and torque generated within each segment. At the same time, it maintains a balance of axial and angular momentum, providing a thorough analysis of the blade interaction with fluid flow [65, 66].

The versatile application of BEMT across both wind and hydrokinetic turbines emphasizes its effectiveness in renewable energy applications, enabling the precise simulation of complex flow scenarios, including variable flow velocities and turbulent wakes. This capacity

is critical for enhancing turbine operational performance, although it requires empirical validation to ensure alignment of theoretical predictions with actual phenomena, highlighting the dynamic nature of turbine design methodologies [9].

Within the QBlade software, BEMT's methodology extends to simulate blade behavior, predict fluctuations in power coefficients relative to tip speed ratio (TSR), and adjust blade pitch. This predictive insight is invaluable during the experimental design phase, helping optimize blade pitch for maximum performance efficacy. Subsequent BEMT simulations within QBlade play a crucial role in validating experimental results, particularly in verifying the effectiveness of designs aimed at minimizing duct contraction ratios while maximizing power coefficients [24, 29].

Furthermore, BEMT emphasizes the importance of adjusting the blade pitch and addressing cavitation problems to improve the overall efficiency of the turbine system. Tailoring pitch adjustments and blade twist according to variable attack angles is crucial for optimal performance, as evidenced by empirical benchmarks such as tow tank tests and evaluations of scaled horizontal axis turbines. These studies confirm BEMT accuracy and applicability by realizing power and thrust coefficient behaviors across different TSRs [9, 47]. Research on the effects of Reynolds numbers on rotor dynamics further accentuates the complexity of accurately modeling turbine performance under varied flow conditions, emphasizing the need to optimize turbine design [35, 47].

As BEMT progresses, the incorporation of more detailed fluid dynamics analyses promises to further enhance turbine efficiency and reliability. Figures 10(a) and 10(b) illuminate the essential angles, velocities, and force components that act on a blade section and outline the iterative process of BEMT simulations, underscoring the comprehensive analytical depth of this theory [66]. This synthesis not only elucidates the dynamic interaction governing blade performance, but also cements BEMT's indispensable role in the continuous development of high-efficiency hydrokinetic turbines [65].

QBlade performs BEMT simulations with the iteration variables, angles, velocities, and

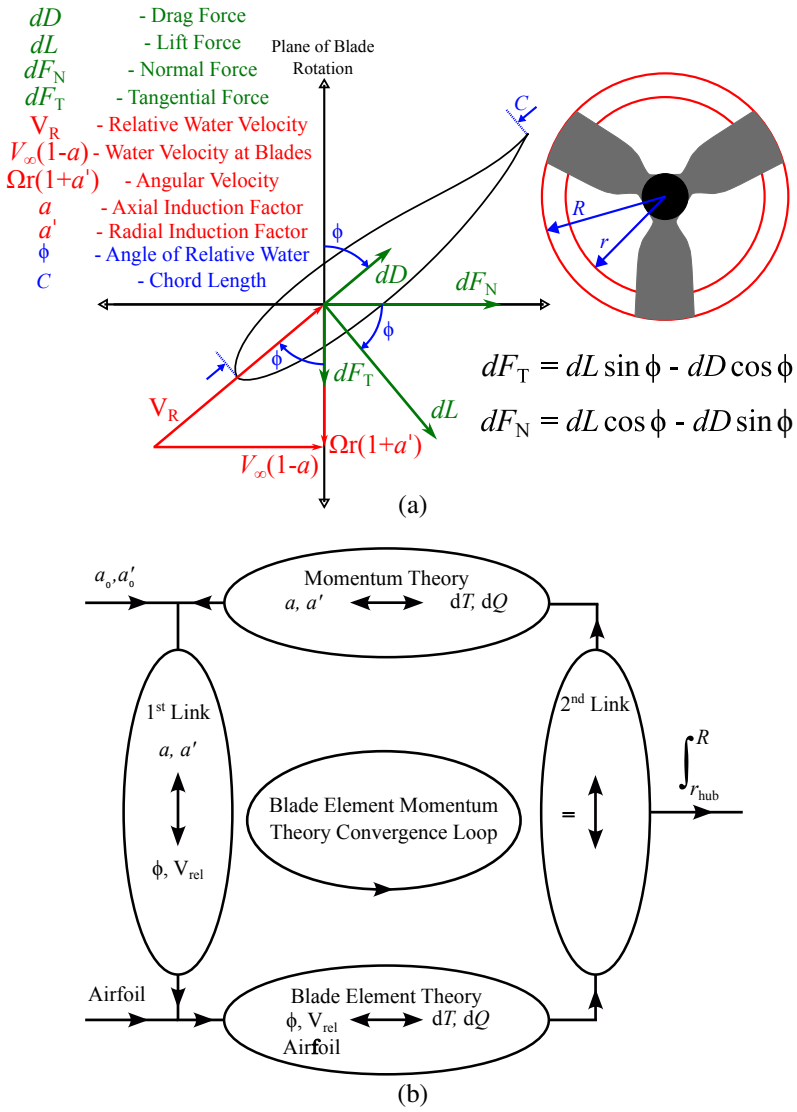

Figure 10: BEMT Analysis (a) Angles, velocities, and force components acting on the rotor blade section [66] b) Iterative process [58]

force components shown in figure 10(a). The iteration variables for this method are the axial (a) and radial (a') induction factors. Angle of attack (α), inflow angle (ϕ), pitch angle (θ), and twist angle (β) are the angles present. The wind velocity at the rotor blade can be seen as V$(1 - a)$ in the horizontal direction. The angular velocity is shown as $\Omega r(1 + a')$. With Fig. 10(a), the inflow

angle and the relative velocity are given by the equations:

$$\phi = \tan^{-1}\left(\frac{V_\infty(1-a)}{\Omega r(1+a')}\right) \tag{1}$$

$$V_R = V_\infty\left(\frac{1-a}{\sin\phi}\right) \tag{2}$$

The chord length (c), number of blades (B), and radius (r) make up the solidity (σ_r) in the following equation:

$$\sigma_r = \frac{Bc}{2\pi r} \tag{3}$$

The solidity ratio represents the fraction of the of the length of the circumference described by the blade tip that is occupied by the blades [43]. Incorporating these ideas produces the axial and radial induction factors seen in:

$$a = \frac{1}{4\sin^2\phi(\sigma_r C_N + 1)} \tag{4}$$

$$a' = \frac{1}{4\sin\phi\cos\phi(\sigma_r C_T + 1)} \tag{5}$$

The normal and tangential force coefficients of the blade section are given by:

$$C_N = C_L\cos\phi + C_D\sin\phi \tag{6}$$

$$C_T = C_L\sin\phi - C_D\cos\phi \tag{7}$$

The iteration technique used in these equations is to first initialize the axial and radial induction factors a and a'. The inflow angle is calculated from (1). The local angle of attack is determined by subtracting the twist angle from the inflow angle. The hydrodynamic coefficients of the tabulated hydrofoil data are used to compute a and a' from (4) and (5), respectively. Then the new axial and radial induction factors are compared with the previous ones. If satisfaction has not been met, the process returns to the second step by recalculating ϕ again. The process is repeated. If simulation satisfaction has been reached within a selected tolerance,

the hydrodynamic loads and the turbine performance are calculated [66]. This complete iterative process utilized in these simulations is simplified in Fig. 10(b).

In general, as well as in QBlade, the power coefficient for a particular turbine is determined with the expression:

$$C_P = \left(\frac{P_{\text{extracted}}}{P_{\text{available}}} \right). \tag{8}$$

This power coefficient utilizes the free stream velocity and the rotor area, producing a power coefficient that abides by the Betz limit of 0.593 [10, 59, 60]. This power coefficient can be corrected, with respect to the entire ducted turbine, by the following expression [67]:

$$C_P^* = C_P \left(\frac{A_{\text{exit}}}{A_{\text{rotor}}} \right). \tag{9}$$

The power available for the fluid is then determined to be [12]:

$$P_{\text{available}} = \frac{1}{2} \rho A_2 v_2^3, \tag{10}$$

where A_2 is the area at the duct throat. With the available power and the power coefficient, the extracted power can be solved for and compared to the experimental results.

3.2 Iterative Experimental Design

This experimental work uses a recirculating open channel flume, shown in Fig. 11, to create controlled water flow in the axial direction of the HAHkT apparatus. The open channel is 4.42 meters long and was modified to include a 1.5 m wide insert where the cross-sectional area of the flow is reduced to 240 by 275 mm, which is intended to increase the initial average velocity of 0.1 m/s. The flume has two 0.75 horsepower pumps that operate at a constant speed of RPM a piece. An aluminum honeycomb core with 3.175 mm cells was used as a flow straightener. An 8.4V 22W waterproof DC motor was utilized as the turbine generator.

For rotor models, blade profile selection, blade count, and intended tip spreed ratio, are

Figure 11: The recirculating open-channel flume located at the University of Memphis

some of the elements that require consideration [7]. An airfoil blade profile that had shown promising results as a hydrofoil was chosen from the National Renewable Energy Laboratory (NREL). [37]. The selected blade profile, NREL S833, is shown in Fig. 12. [29] performed ANSYS simulations on the NREL S832, the neighbor to S833, for flow separation characteristics, providing insight into its robustness against varying angles of attack, suggesting that it is a preferable choice for blade design in hydrokinetic turbines. This provides further confirmation that the S833 is a hydrofoil worthy of exploration. The rotor models consisted of three blades as this is the most widely utilized and balanced option when considering TSR, power coefficients and manufacturing costs [7].

With the slow average velocity potentially becoming problematic for experimentation, it was determined that an initial test was needed. Figure 13(a), (b), and (c) display the initial apparatus assembly which was secured to the flume at the base and to a metal rod through slots on the top portion. This initial test assembly was used to direct the full flow of the flume through the turbine area, providing a proof of concept and initial flow rate data necessary to perform more accurate simulations and therefore a better design. The maximized flow gave a Reynolds number close to 60,000 at the tip of the blade. It is assumed that the water flow is incompressible and resides within the transitional regime because of the expected range of Reynolds numbers. Although flow separation could potentially be observed at higher angles of attack, the operational

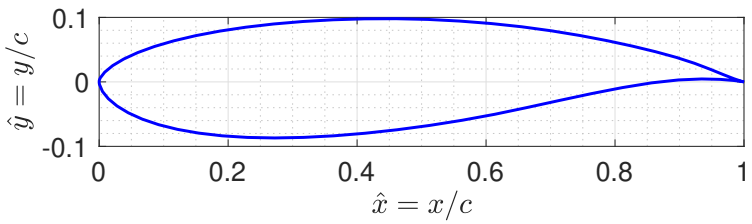

Figure 12: Normalized Profile of NREL S833 Hydrofoil

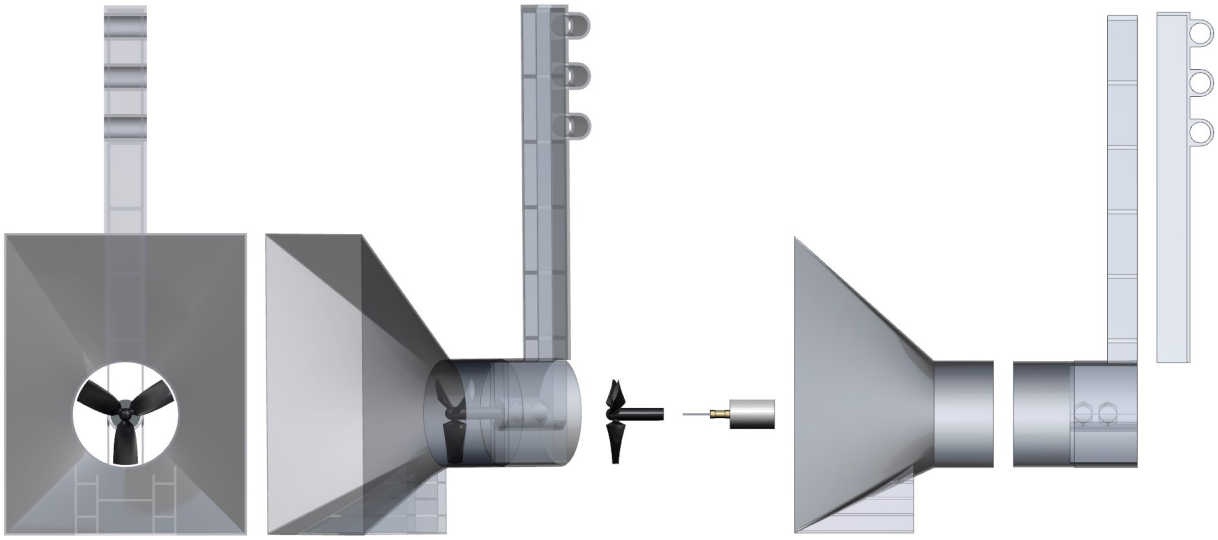

(a) (b) (c)

Figure 13: The proof of concept design (a) Front view (b) Angled assembled view (c) Exploded side view

range avoids the stall regime of the blade profile.

To find a suitable initial angle of attack α, XFOIL analyses were performed in QBlade from $-20°$ to $+20°$ with a Reynolds numbers representing the root of the blade, the middle section of the blade and the tip of the blade. It is essential for the Reynolds number to reflect the operating range of the foil to be modeled to appropriately determine the lift and drag data [68]. The corresponding Reynolds numbers were rounded to the nearest $10,000$ to produce $20,000$, $40,000$ and $60,000$, respectively. The results of these analyses are shown in the next chapter.

With these XFOIL results, the angle of attack (α) of 7° was chosen as a baseline angle of attack (α_0) for the expected Reynolds number range. Figure 14 shows the angle of twist, β, for the idealized ducted rotor model. β, for the blade sections was calculated with the following

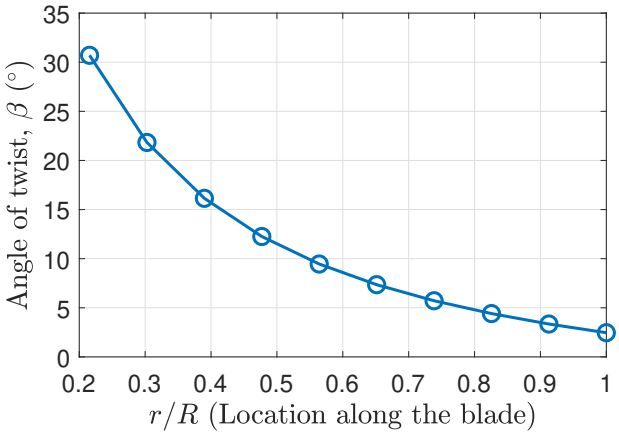

Figure 14: Angle of twist designed as a function of normalized radius along the blade

relationship:

$$\beta = \tan^{-1}\left(\frac{U}{r\omega}\right) - \alpha_0, \tag{11}$$

where U is the nominal velocity, which was initially set to 0.678 m/s, ω is the nominal rotational speed, which is set to 30.5 rad/s, and r is the distance along blade which began at a radius of 6.42 mm and increased by increments of 4.36 mm till the tip at 50 mm. This ensures that all local blade section locations have the baseline angle of attack at the nominal flow speed and the optimal TSR [53] when the controlled blade pitch (θ_p) is maintained at $0°$. The TSR of the initial test was on the lower end at 2.25. This was calculated with the following relationship:

$$\text{TSR} = \left(\frac{r\omega}{U}\right). \tag{12}$$

For a three-blade turbine, the optimal TSR is near 5 [69]. Ducted hydrokinetic turbines operate more efficiently at higher TSR values than their bare counterparts [70, 71]. Caviation typically occurs at TSR values greater than approximately 7 [72]. With these elements in mind, the design TSR of 6 was selected as the idealized ducted TSR on which the β for the final rotor models would be based. The first iteration of the rotor models was designed to optimize β to maximize power in an effort to determine the "mechanical" resistance of a rotor. U and ω were then set

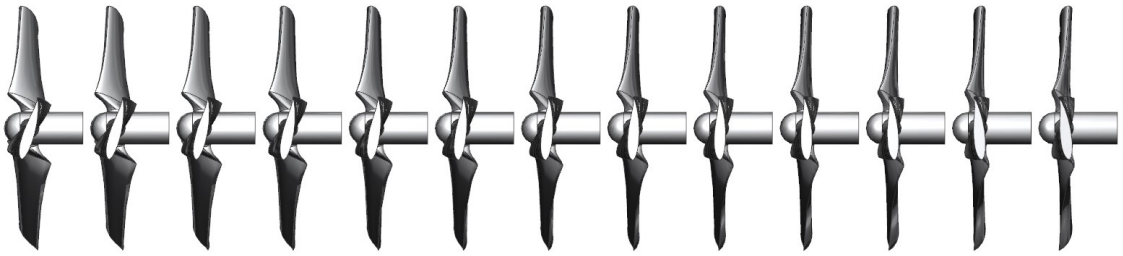

Figure 15: Three-dimensional rotor model pitches from -12° to 12° in increments of 2°

at 0.34 m/s and 40.8 rad/s, respectively, in order to produce this idealized TSR. The blade tips for all rotor models were slightly trimmed so that the tip clearance was 2 mm for every pitch. Varying tip clearance was not explored, but its understanding is essential for ducted turbine efficiency.

Figure 15 shows the side view of the 13 rotor models from pitch -12° to $+12^\circ$ in increments of 2° . For simplicity, the chord was kept constant at 25 mm throughout the blade with the NREL S833 profile up to the point where it converged to a circle of 7.5 mm diameter. The potential optimization of the chord with a one-dimensional analysis has been shown to be a viable method to avoid cavitation [73]. However, changes in chord, cavitation, tip clearance, and generator control were not explored in this experiment, but are essential to incorporate for full control design optimization.

After the initial test was performed, the final designs of a small-scale ducted HAHkT were created for use in the open channel flume. These final designs consisted of various components that were printed, constructed, and procured. The equipment required consisted of the following items and printed models: a brushed waterproof DC motor acting as a generator, a voltmeter, an ammeter, a flow meter, a slow motion camera, a thermometer, 13 different rotor models varying in collective pitch from -12° to $+12^\circ$ in increments of 2° , and three ducts with duct contraction ratios 1, 0.75, and 0.5.

The 13 different rotor designs, each with a different fixed pitch, and three ducts of varying duct contraction ratios were designed in Siemens NX and printed in polymer, polyethylene

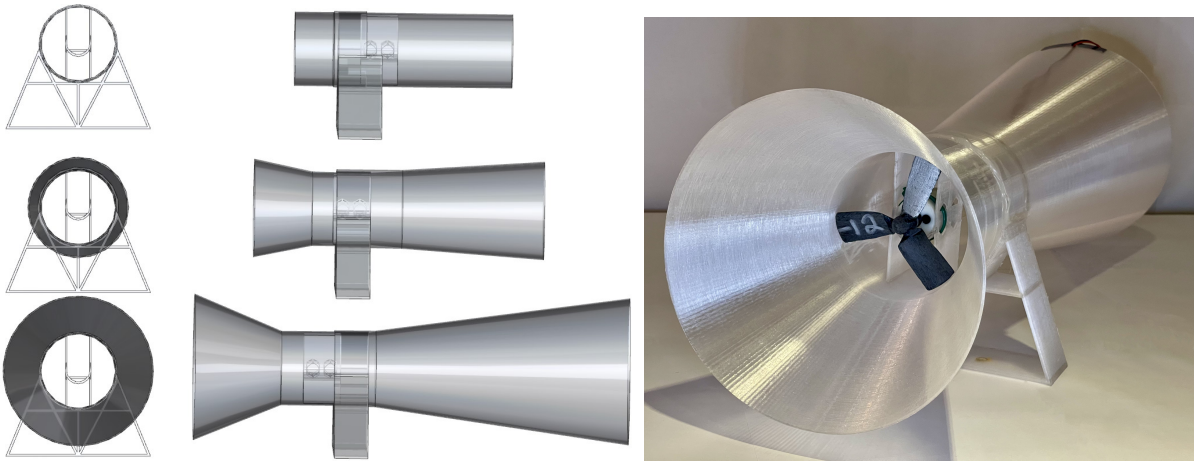

(a) (b) (c)

Figure 16: Final duct models and printed assembly (a) Model front view (b) Model side view (c) Complete printed assembly featuring duct with CR=0.5 and pitch of $-12°$

terephthalate glycol (PETG), through a fused deposition material (FDM) process. PETG was chosen because of its strength and hydrophobic characteristics. The Creality FDM printers utilized were the CR-M4 and Ender V3 SE. The CR-M4 printed the duct pieces due to its large printing volume; however, due to the length of the entire ducts, each duct had to be printed in two pieces. For duct contraction ratios of 0.5 and 0.75, the divergent nozzle was printed separately from the turbine area and the divergent nozzle. Due to the reduction in total length for the duct contraction ratio of 1 and the fixed length of the rotor and motor, the motor holder had to extend into the divergent nozzle so that the tip of the rotor would not exceed the entrance of the convergent nozzle. Therefore, the convergent nozzle was printed separately from the turbine area and the divergent nozzle for the duct assembly with the duct contraction ratio of 1. The ducts were all printed in clear PETG with 110% flow and a nozzle diameter of 0.8 mm in attempt to create a translucent finish. The rotor models were printed in black PETG with 98% flow and a nozzle diameter of 0.4 mm. Both printers were used to print the rotor models at the 13 different pitches. All printed models required some sanding to remove excess support material and refine the surface.

The duct designs followed the following ratios from Bilgen et al. [12]: aspect ratio of

6, inlet-to-outlet diameter of 1, and contraction ratios of 1, 0.75, and 0.5. These designs were originally implemented under the guise of a previous goal, but were essential in the goal of DCCS formulation. With the size of the flume, average speed of the flume, and the need to explore multiple contraction ratios all taken into consideration, a simple CFD analysis was performed pre-experiment with the largest duct with contraction ratio of 0.5. The boundary layer was determined to be negligible due to its small magnitude. This confirmed that the largest duct would not encounter adverse boundary layer effects from the flume walls.

Figures 16(a) and 16(b) show the final computer aided designs for each of the printed and tested duct assemblies. Figure 16(c) is a photo of the largest, duct assembly with CR of 0.5 and rotor with blade pitch of $-12°$. In order to secure the duct assembly, the turbine base was screwed into anchor sockets on the base of the flume, and the motor wires were secured to the divergent nozzle end and to the top wall of the flume, placing an upward force on the divergent end that counters the upward force on the convergent end from the incoming flow. Rotor pitch models were adhered with hot glue to a coupler located on the motor shaft. To change the rotor pitch model that was being tested, a heat gun was applied momentarily to the attached rotor, allowing the glue to melt and the rotor to be removed.

Lastly, the flow generated from the pumps was constant, and therefore the flow was assumed to be steady. The primary objective of the experiment was to collect data on the rotational speed of the rotor, the output voltage, and the output amperage for various duct contraction ratios and blade pitches. Without any efficiency information, the power extracted is equated to the electrical output. This collection of data is essential to formulate the experimental power coefficient with the relationship in Eq. (8).

The steady flow of the free stream after the flow straightener and submerged recording device, but before the entrance of the duct, was measured five times with the portable FM-100V5 flow meter at the start of every pitch trial. This flow meter has a speed range of $0.01 - 5.00$ m/s with a current measurement error less than or equal to 1.5%.

The flow temperature for simulation purposes is considered to be a constant $20°$ C,

however the temperature for the final experiment was monitored with a Goodcook thermometer to ensure that the heat produced by the pumps did not drastically vary the temperature, which would affect the viscosity. This thermometer has an accuracy of $\pm 1^{\circ}$C. At the beginning and end of each pitch trial for each contraction ratio, the temperature was taken in three areas of the flume. In large deep-sea applications, temperature gradients can lead to thermal stratification, possibly having a substantial effect on turbine wake stability, which is necessary to understand for efficient deep-water turbine farm arrays [51], although not explored in this paper.

The voltage was measured three times per single pitch test. The Omega data logger, used as a voltmeter to read millivolts, records 125 samples per second and has an accuracy of $\pm 1\%$ of the full scale. The current was measured four times per pitch test in milliamps with the XL830L multimeter, which has an accuracy of $\pm 1.5\%$. Current and voltage were measured separately to avoid dividing the voltage across the ammeter resistance.

These results are later compared with the simulated results, and the validity of the optimal design parameters will be determined. The C_P can be corrected to find the value of the power coefficient associated with the entire duct, which abides by the Betz limit, using the same relationship previously mentioned in Eq. (9). The final average results for each CR were then used in the creation of the surrogate model (SM).

3.3 Duct Contraction Control Strategy Formation

The formation of DCCS is a key development in the pursuit of optimizing the hydrokinetic energy system. Using a surrogate model based on detailed experimental data, the strategy dynamically adjusts turbine settings in response to changing flow conditions, markedly improving power output. This adaptive approach was rigorously tested across various velocity profiles, demonstrating its potential to significantly enhance the economic viability of hydrokinetic turbines by reducing the Levelized Cost of Energy (LCOE). The DCCS represents a major leap in hydrokinetic turbine technology, offering a more flexible and efficient solution to energy extraction challenges. The strategy's development involved comprehensive simulation and

optimization processes, employing advanced numerical methods to refine turbine performance and efficiency. By integrating real-time data and predictive modeling, the DCCS enables a more responsive and effective energy production system, setting a new standard for renewable energy technologies. This innovative control strategy not only advances hydrokinetic turbine efficiency but also contributes to the larger goal of sustainable and reliable renewable energy solutions, highlighting the importance of dynamic control systems in the future of energy technology.

3.3.1 Surrogate Modeling

The next step in improving ducted HAHkT systems involves leveraging data from water flume experiments to develop a SM with the open source surrogate modeling toolbox. The Kriging method, which performs regression and interpolation with experimental data to create a function for power and angular velocity as the blade pitch and the rotor area velocity are varied, was utilized to create this SM. The interpolation results of the Kriging method have been shown to be very effective because it is unbiased and has minimum estimation variance [74–76], thus this method is generally selected in the surrogate model of the simulation model [74, 77–81]. This SM serves as a dynamic reduced order model (ROM), intricately designed to capture the complex interactions of varying duct contraction ratios and blade pitch adjustments under different flow conditions. The primary goal was to use this ROM to design the DCCS that ensured optimal power output.

Traditional design methodologies face challenges due to the absence of simple and validated models suitable for system-level optimization tasks. Existing models often rely on computationally intensive computational fluid dynamics (CFD) simulations or ROMs that have not yet been validated, restricting their applicability across various flow conditions [12, 67, 82]. Although ROMs offer computational efficiency, their effectiveness in optimizing dynamic system design remains constrained by the complexity of the optimization problem [12, 83]. However, significantly lowering computational requirements can facilitate practical engineering assessments of turbine performance and reliability [9]. Therefore, it is paramount to advocate for

Table 1: Summary of Cases with Applied Constraints

Case	Velocity Profile	ΔCR Con.	ΔPitch Con.
1	$0.4 + 0.3 \cdot \sin(\frac{2\pi}{60}t)$	± 0.01175	± 3
2	$0.4 - 0.3 \cdot \exp(-\frac{t}{60}) \cdot \sin(\frac{2\pi}{45}t)$	± 0.011	± 3
3	`numpy.random.seed(42)`	± 0.01	± 0.5
4	`numpy.random.seed(46)`	± 0.025	± 5.0

a SM as a ROM, especially when it is experimentally validated, as it is in the DCCS.

3.3.2 Design Optimization

Energy extraction efficiency in hydrokinetic systems is directly influenced by the density of the fluid, the cross-sectional area of the flow, and the velocity of the water, highlighting the need for optimized hydrodynamic and mechanical designs [4]. Luquet et al. (2013) demonstrated through numerical simulations and model testing that an optimized duct and rotor design can achieve a high power coefficient of 0.75, confirming the efficiency of ducted marine current turbines [8]. To achieve improved results similar to these, the plan incorporated the use of OpenMDAO, an open source framework for performing multidisciplinary analysis and optimization [84], to optimize the SM. The optimization process aimed to maximize power generation by dynamically adjusting the blade pitch and duct contraction ratio based on velocity profiles that resembled real-time oscillating inflow conditions. This strategy allowed for the balance of energy production with operational considerations, ensuring a sustainable and efficient approach.

The OpenMDAO framework with the IPOPT optimizer takes into account the empirically supported SM as a map, the input of the water velocity profile, and the duct contraction ratio rate and pitch rate constraints to provide the optimal time variant solution. Unconstrained optimizations were also explored for comparison. The Gulf Stream core speed is 2 m/s [85], however, this exceeds the limits of the SM. Therefore, a lower magnitude of velocity profiles

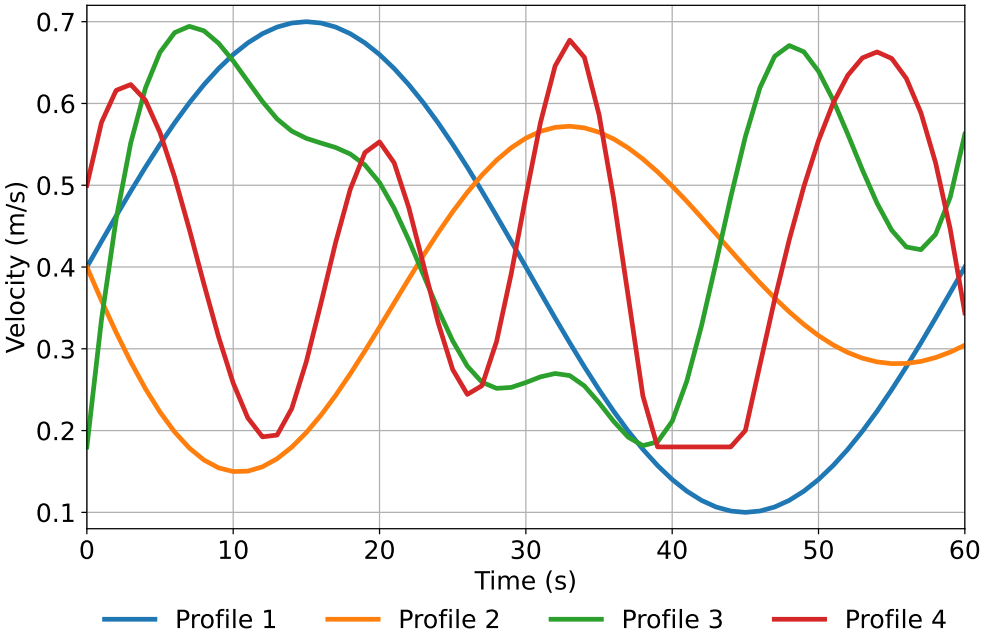

Figure 17: Velocity Profiles for Design Optimization

was used for the optimization tests. The parameters chosen for each design optimization case are shown in Table 1. The exact velocity profiles can be seen in Fig. 17. Velocity profiles 1 and 2 are simple sinusoidal and damped sinusoidal, respectively. Velocity profiles 3 and 4 are uniformly random generated profiles with Numpy's random seeds 42 and 46 respectively. These profiles represent a range of potential flow behaviors that are limited within the range of the experimental minimum speed of 0.18 m/s and the experimental maximum speed of 0.72 m/s.

By comparing the optimizer's paths under these varied conditions, a comprehensive understanding of the system's performance and adaptability can be achieved, ensuring that the ducted HAHkT system operates at peak efficiency across a range of scenarios. This streamlined approach marks a significant advance in the field of hydrokinetic design with the goal of optimizing energy production.

3.3.3 Constraint Analysis

The constraint coefficient, γ, is multiplied to the lower and upper bounds for duct contraction rate and blade pitch rate, given as:

$$\left|\dot{\mathrm{CR}}\right| \leq \gamma \cdot \dot{\mathrm{CR}}_{\mathrm{max}} \tag{13a}$$

$$\left|\dot{\theta}_{\mathrm{b}}\right| \leq \gamma \cdot \dot{\theta}_{\mathrm{b,max}}, \tag{13b}$$

where $\dot{\mathrm{CR}}$ is rate for duct contraction ratio, $\dot{\theta}_{\mathrm{b}}$ is rate for blade pitch, and subscript max denotes the predefined limits for the corresponding quantities. When γ approaches zero, duct contraction and blade pitch control become fixed, making them ineffective. On the contrary, as γ approaches infinity, duct contraction and blade pitch control respond immediately to environmental changes (water flow speed), producing maximum theoretically achievable power. A practical value for γ typically falls within the range of around 1, allowing finite rates for controller actuation.

In the constraint analysis, the average power output of the HAHkT varied with different levels of constraint applied to the DCCS. γ was used to modulate the degree of constraint, enabling a systematic exploration of turbine performance under varying operational limitations. In this investigation, the mechanisms required for controlling the actuation of the duct and rotor blades are not explicitly considered. However, it acknowledges that realistic actuation rates must be achieved, as actuation cannot occur instantaneously. This consideration is crucial for applying the findings to real-world scenarios, where mechanical and system limitations can restrict rapid adjustments in turbine settings.

The incremental adjustment in this analysis of γ, directly influenced the rate at which the CR of the duct and the pitch of the blade could change. This approach allowed observation of the turbine power output response to different rates of operational change, effectively simulating real-world scenarios and highlighting the importance of considering actuation dynamics in the DCCS design.

To fully understand the effectiveness of the proposed strategy with duct contraction and

pitch control, the scenario for Case 4 was compared with a scenario where only pitch control was used with a constant duct CR of 1. This comparison isolated the impact of duct contraction adjustments on the overall power efficiency of the turbine system. Inclusion of actuation considerations further emphasizes the need for realistic, implementable control strategies in the optimization process.

By methodically varying the constraint coefficient and observing the corresponding power output, the analysis provided insight into the optimal balance between operational flexibility and power efficiency. The methodology identified the efficiency peak where the turbine operates effectively without being overly restricted by operational constraints. This insight is instrumental in forming the design and operational strategy for DCCS implementation in HAHkT systems, ensuring that control mechanisms are both effective and realistic in their actuation capabilities.

Chapter 4

Results and Discussion

The validation of ducted turbine designs requires a combination of analysis, calculation, and experimentation, highlighting the multifaceted approach needed to optimize these systems [8]. These experimental and simulated results represent the culmination of efforts to create and explore the duct contaction control stategy (DCCS).

4.1 Experimental Results

The initial experiment was performed with only 4 different pitched rotors and one total convergence nozzle. In addition, a braking resistance was applied in each test in order to determine if angular velocity could be controlled by generator means. The results of this initial test can be seen in Fig. 18. For this specific blade design, the pitch of 6° was found to produce the most power. The attempts to apply a braking resistance were a failure, since the video footage analyze provided no difference between applied resistances, leading to the belief that the internal motor's resistive force was negligible in comparison to the force from the flow.

The initial test influenced more simulations, a redesign of the rotor blade for overall reduction of the rotor length, a twist created with a design tip speed ratio (TSR) of 6, and a duct redesign for material reduction and proper securement. After the printing of all updated parts was complete, four tests were carried out for each pitch trial for each contraction ratio (CR). The average water speed was determined to be 0.18 m/s. For CRs 1, 0.75, and 0.5 the inflow speeds are assumed to be 0.18 m/s, 0.32 m/s, and 0.72 m/s, respectively, in accordance with continuity.

The results for each CR corresponding to 1, 0.75, and 0.5 are shown in Figs. 19(a), (b), and (c) respectively. In these graphs, the mean value, range, and 95 percent confidence interval are identified for each pitch trial. It can be seen that the design was more effective at a collective pitch of -2° for the the lowest CR which corresponds to the highest throat velocity. This implies that the blade design could be altered again such that the 0° produces the most power. These

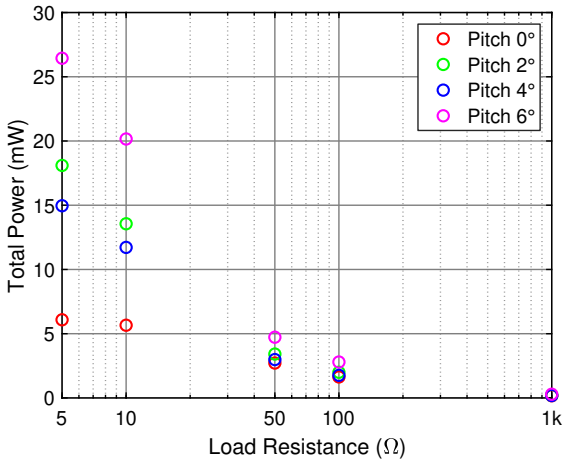

Figure 18: Power results for the total convergence tests at various rotor pitches and load resistances

results also produced pitches that were inoperable. It should be noted that a pitch of $12°$produced stall for all duct contraction ratios. Combining the average power results of the three complete CR tests, seen in Fig. 19(d), provides a dynamic representation of the power and angular velocity influenced by pitch and CR.

The highest values calculated for variance were 1.2, 0.52, and 0.35. Since the results for Z-score and IQR Method were within the bounds, there were determined to be no outliers. The method applied to quantifying the uncertainty in experimental measurements, including instrument calibration, ensures a high degree of confidence in the data obtained from the tests [47]. The uncertainty of the instrumentation is contributed by the uncertainty associated with the flow meter, the ammeter, and the data logger utilized as a voltmeter. Statistical uncertainty was determined for each individual duct. For CR=1, CR=0.75 and CR=0.5 the uncertainty was 3.27 ± 0.01, 5.73 ± 0.02, and 23.7 ± 0.06, respectively. The high repeatability of the results confirmed by uncertainty analysis demonstrates the ability of a test apparatus to provide consistent and accurate performance data for turbines [47].

The temperature per pitch trial varied on average $0.26°$ C and the maximum variation was $0.94°$ C. The total temperature ranged from $16.3°$ C to $21.7°$ C for the entire experiment. Efforts were made during the experiment to minimize the temperature change by introducing

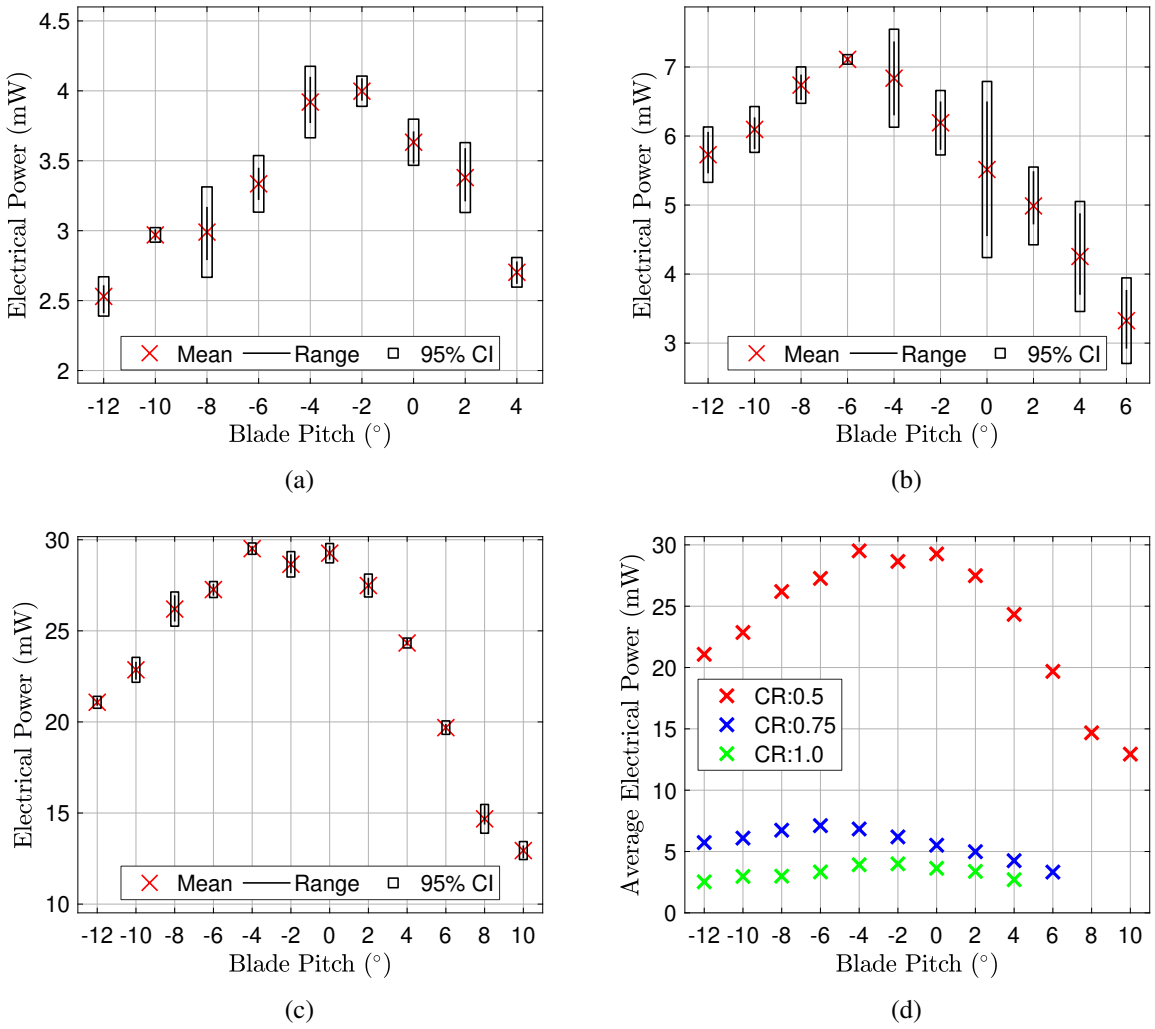

Figure 19: Experimental electrical power results as blade pitch and duct contraction ratio are varied. (a), (b), and (c) Individual power results for duct contraction ratios equal to 1, 0.75, and 0.5. (d) Cumulative average power results.

cold water while draining existing water while also trying to maintain a nearly constant volume of water in the flume.

4.2 QBlade Results

QBlade analyses were instrumental in pre- and post-experimental evaluations. The results of the XFOIL analysis corresponding to the Reynolds numbers, from root to tip, are shown in

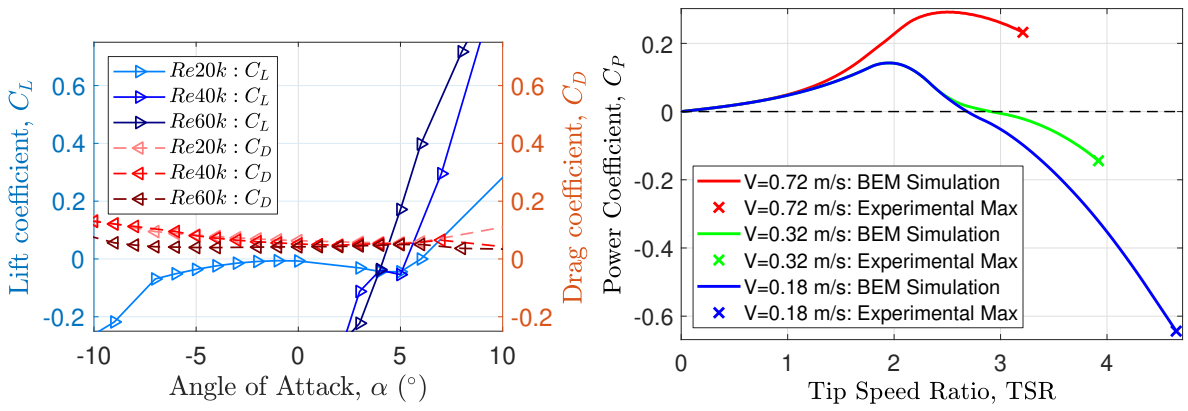

(a) (b)

Figure 20: QBblade simulations (a) Angle of attack pre-design results (b) BEMT simulation post-experiment results for constant velocity at collective pitch of $-2°$

Fig. 20(a). It can be seen that certain points were not recorded due to stall. Previous work using NREL S833 at higher Reynolds numbers came to the conclusion that $6°$ is the ideal α [86]. However, in the figure it can be seen that the drag coefficient exceeds the lift coefficient at $6°$ for a Reynolds number of $20,000$ and should therefore be excluded. With this in mind, α of $7°$ was chosen as a baseline angle of attack (α_0) for the expected Reynolds number range. This effort to determine a design α was made to maximize the lift while preventing stall.

QBlade Blade Element Momentum Theory (BEMT) rotor simulations were performed at the inflow speeds corresponding to the expected throat speed of each duct contraction ratio and a collective pitch of $-2°$, since it was the optimal pitch for the duct CR that produced the most power experimentally. These BEMT simulations were terminated on the TSR corresponding to the TSR obtained from the experimental data of the maximum angular velocity for each CR. The results of these simulations are shown in Fig. 20(b). These express that for the rotor design, lower operational TSRs are more optimal, but so are higher inflow speeds. It also verified that imploring the lowest CRs produced better power coefficients as the inflow remained constant and the radial speed varied. Negative power coefficients were the result of TSR regimes in which the rotor consumes energy rather than generating it, comparable to that of a propeller. The only way

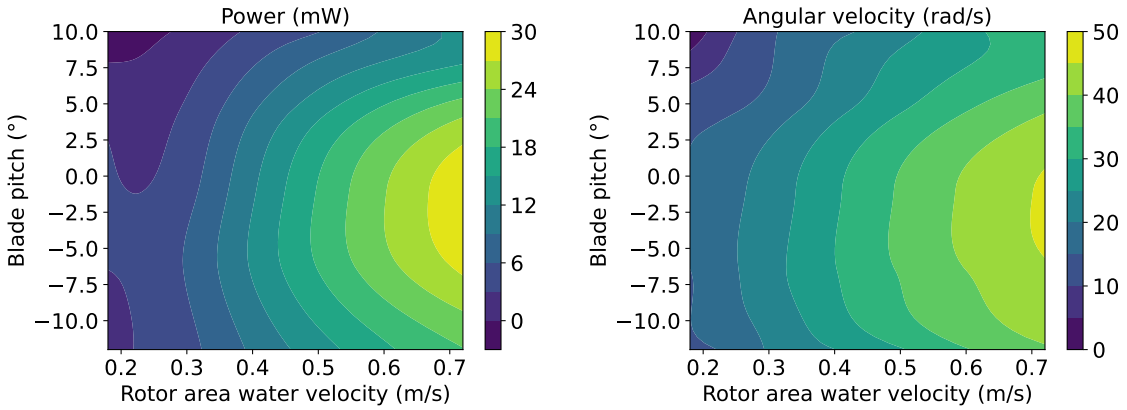

(a) (b)

Figure 21: Surrogate models produced from experimental data. (a) Power distribution as a function of blade pitch and rotor area velocity. (b) Angular velocity distribution as a function of blade pitch and rotor area velocity.

Table 2: Summary of Optimal Solutions

	Average Power (mW)	
Case	**Constrained Case**	**Unconstrained Case**
1	20.30	26.73
2	23.21	28.76
3	20.92	29.15
4	21.50	29.15

these coefficients of power can be improved is by reducing the drag coefficient, which improves the glide ratio by means of either thinning circular sections or increasing the Reynolds number. This opens the door to exploring CR values between 0.5 and 0 since the Reynolds number will undoubtedly increase within this regime.

4.3 Duct Contraction Control Strategy Case Study

Figures 21(a) and (b) display the surrogate model (SM) created using the open source surrogate modeling toolbox. This SM maps power in 21(a) and angular velocity in 21(b) as functions of blade pitch angle and rotor area water velocity. The average experimental power

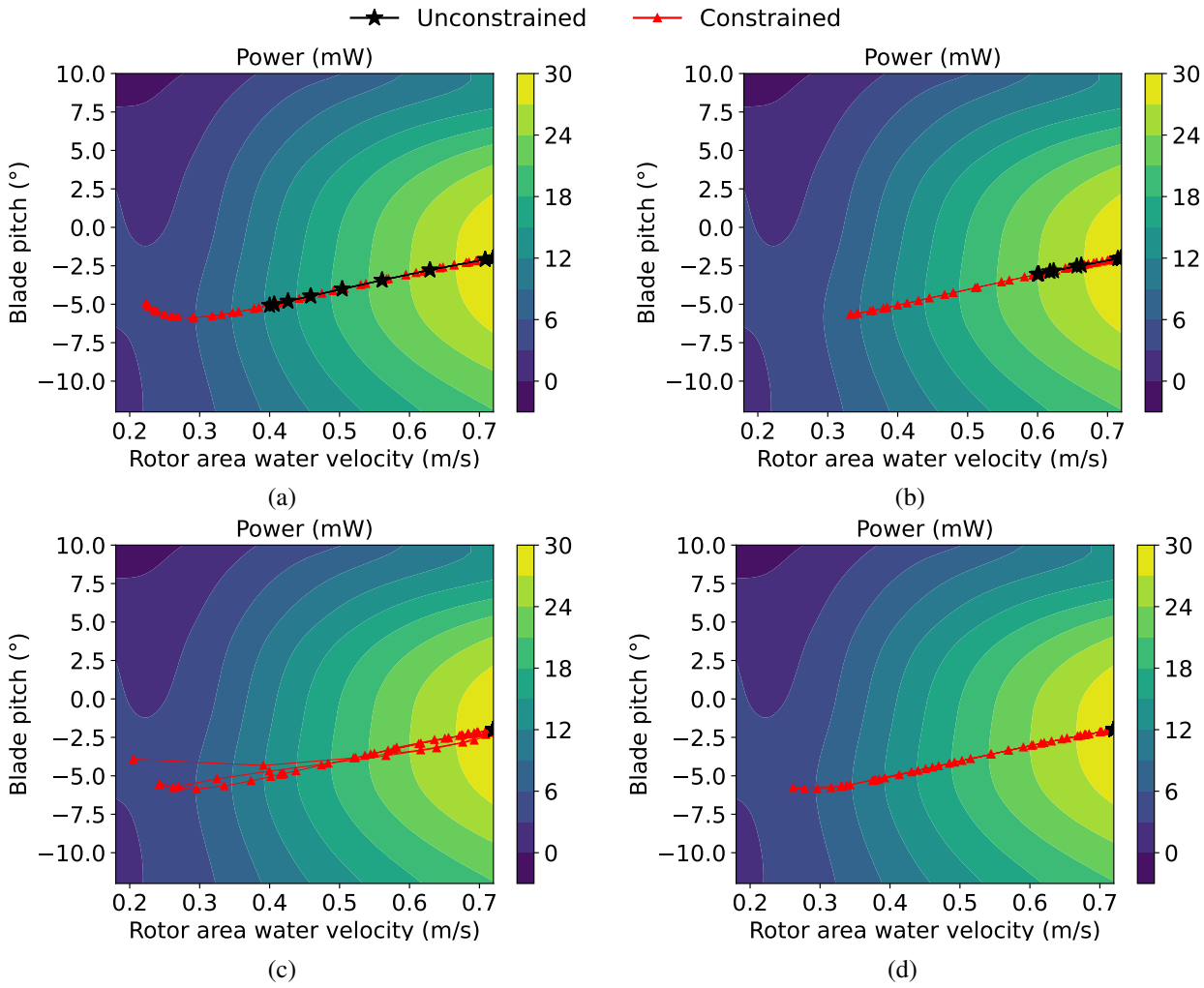

Figure 22: Constrained and unconstrained design optimization results for various velocity cases. (a) Optimal response to sinusoidal velocity profile. (b) Optimal response to the sinusoidal damped velocity profile. (c) Optimal response to the uniform random velocity profile created with random seed 42.(d) Optimal response to random uniform velocity profile created with random seed 46.

results, previously shown in Fig. 19, were the static points utilized to map the behavior and bounds of this model. These maps show that a pitch of -2° and a water velocity of 0.72 m/s provide the optimal power and angular velocity.

The average power results for the four constrained and unconstrained optimization cases can be found in Table 2. The unconstrained cases all obtained near-rated power. Cases 1 and 2 could not achieve rated power due to the velocity profile not allowing for this at the low speeds

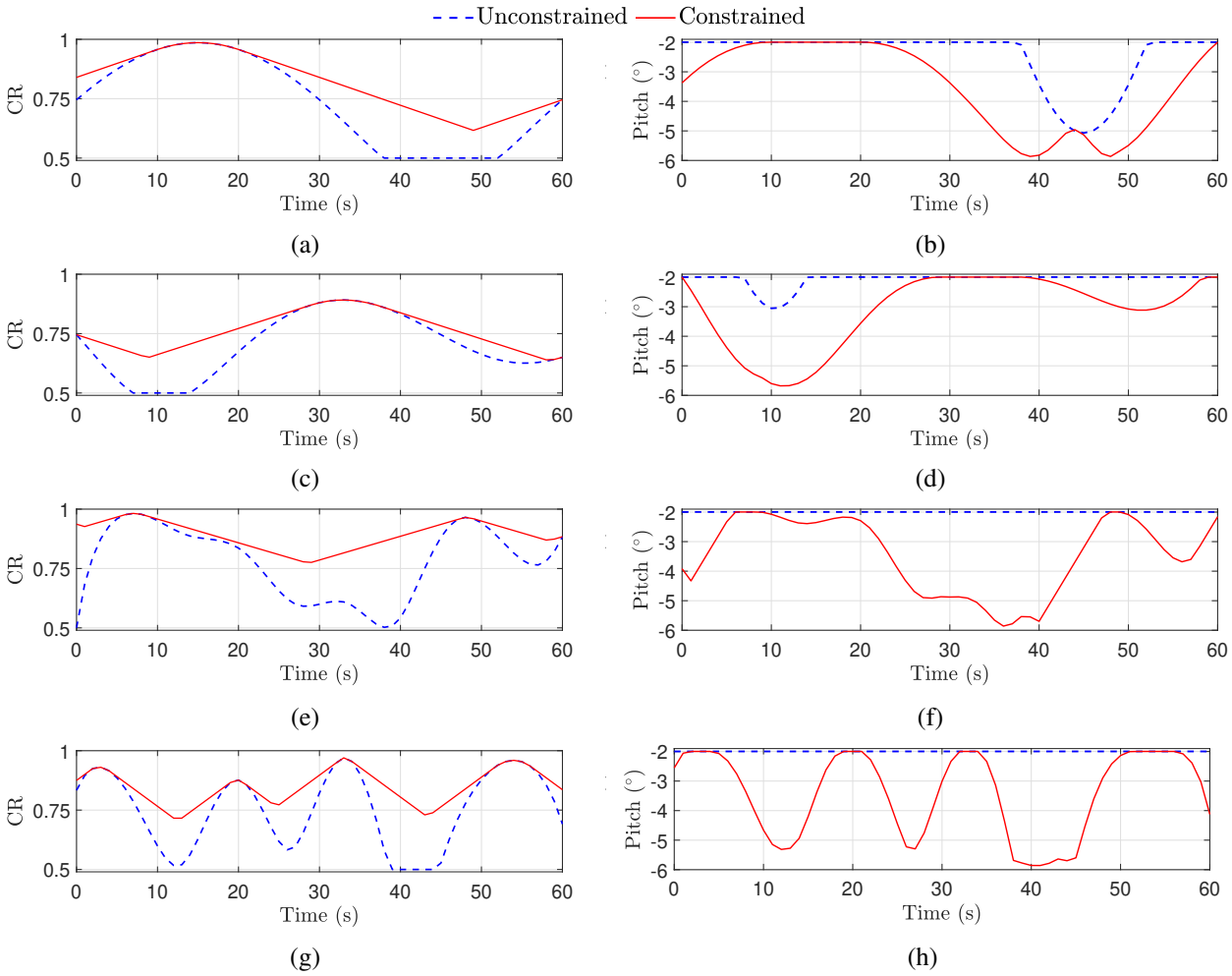

Figure 23: CR and Pitch results of constrained and unconstrained design optimization at various velocity cases. (a), (c), (e), and (g) Optimal CR as a function of time for velocity profile 1, 2, 3, and 4 respectively (b), (d), (f), and (h) Optimal CR as a function of time for velocity profile 1, 2, 3, and 4 respectively

that were unable to be corrected to the maximum rotor velocity of 0.72 m/s. The constrained cases did not obtain average maximum power; however, these represented realistic constraints that would only allow for pitch and CR to change at a realistic rate in a given window of time.

Figures 22(a)- (d) depicts the constrained and unconstrained results for design optimization for each of the cases. Cases 1 and 2 in Fig. 22(a) and Fig. 22(b) both show instances where the duct contraction ratio could not bring the water to optimal speed, yet optimal results were always attained for even the slow water speeds. Case 3 and 4 in Fig. 22(c) and Fig. 22(d),

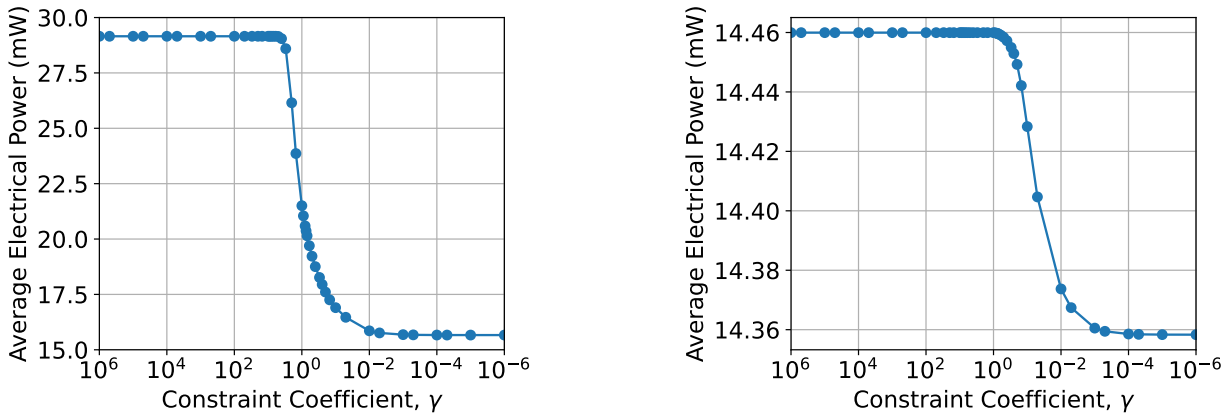

(a) (b)

Figure 24: Constraint Analysis for Case 4 where the water velocity profile spans the minimum and maximum experimental velocities of 0.18 m/s to 0.72 m/s (a) Duct contraction control and pitch control (b) Pitch-only control and constant contraction ratio of 1

where more chaotic velocity functions were implored, the constrained optimization can be seen slightly struggling to stay in the optimal region, while the unconstrained optimizations attained optimality for the entire duration of the simulation. In Fig. 22(a) and Fig. 22(c) the pitch control can be seen responding at very low water speeds in an attempt to maximize energy when the duct is fully expanded and cannot further affect the water speed.

Figures 23(a)-(h) displays the dynamic CR and pitch response for all velocity profile cases, constrained and unconstrained. It is clear that as CR struggles to compensate either due to very low inflow or constraints, the pitch is adjusted instead to match the velocity profile. Otherwise, the pitch remains near the optimal location of -2° . It can also be seen that the unconstrained CR profiles have no issue in conforming to the velocity profile in order to produce maximum power.

Figures 22 and 23 clearly demonstrate the substantial influence of duct contraction control on recovering and maintaining maximum power output when possible. Duct contraction control is seen to be the sole contributor to significant power deviations in idealized unconstrained cases. The pitch control for all cases, constrained and unconstrained, acted as a

Table 3: Summary of Constraint Analysis for Case 4

Case	Average Power (mW)	
	Minimum	**Maximum**
Duct Contraction and Pitch Control	15.08	29.15
Pitch-only Control and Fixed CR of 1	14.43	14.53

secondary control when the duct contraction control could not suffice.

Figure 24 illustrates the relationship between overall power production and the levels of rate constraints applied in the design optimization case 4. Figure 24(a) displays the results of the proposed duct CR control and pitch control. It can be seen that a realistic initial constraint for the DCCS was chosen as γ of 1, between the minimum and maximum power. Figure 24(b) displays the results of a constant CR of 1 and pitch-only control. It can be seen that a realistic γ for the pitch-only case is around 0.1, between the minimum and maximum power. The DCCS is particularly notable for generating higher average power and offering a broader range of achievable output powers compared to the scenario with only pitch control and a fixed CR of 1. The summary of the constraint analysis in Table 3 displays the range of power achievable by the DCCS, with duct contraction and pitch control, compared to the range of power achievable with pitch-only control and a fixed CR of 1. In this comparison, the impact of the duct contraction control, in addition to the pitch control, is evident. In ideal, unconstrained scenarios, the DCCS has nearly double the average power in comparison to pitch-only control and a fixed, straight duct. Even in the most heavily constrained scenarios, corresponding to a minimum power of 15.08 mW, the DCCS outperforms pitch-only control unconstrained with a maximum power of 14.53 mW.

Chapter 5

Conclusion

This research marks a pioneering venture in the realm of renewable energy, introducing the duct contraction control strategy (DCCS) for ducted horizontal axis hydrokinetic turbines (HAHkT). This novel contribution signifies a transformative leap in the optimization of hydrokinetic turbines, combining dynamic control of duct contraction ratios (CR) and blade pitch with real-time aquatic conditions to maximize energy extraction efficiency. The development of the DCCS, underpinned by rigorous empirical testing and advanced simulation through QBlade software, showcases its potential as a groundbreaking control mechanism, enhancing the performance predictability and operational adaptability of HAHkT systems.

Experimental investigations and surrogate model analyses have underscored the DCCS's capacity to dynamically adjust turbine operations, thereby optimizing power output across varying flow conditions. This adaptability was substantiated through extensive open-channel water flume experiments, affirming the efficacy of DCCS in real-world scenarios. The strategic integration of duct contraction and pitch control mechanisms within the DCCS framework has demonstrated a significant enhancement in power generation capability, surpassing the limitations of fixed duct systems and pitch-only control strategies.

Analysis of duct contraction and pitch control constraints versus pitch-only control revealed the superior adaptability and efficiency of the DCCS. The constraint analysis illustrated that the DCCS, coupled with pitch control, provides a broader operational range to achieve optimal power output, showcasing its superiority over traditional systems with fixed CR and isolated pitch adjustments. This comprehensive control approach, validated experimentally, not only exemplifies a significant advance in turbine design optimization but also establishes the DCCS as a first-of-its-kind strategy in the hydrokinetic energy domain.

5.1 Advancements and Broader Impact

The introduction of DCCS heralds a significant advancement in the field of hydrokinetic energy, representing a novel and dynamic approach to optimizing turbine performance. Through its innovative integration of adaptive control systems, the DCCS has the potential to revolutionize the design and operation of hydrokinetic turbines. By enabling adjustments to both the duct contraction ratios and the blade pitch, the DCCS significantly improves the adaptability and efficiency of hydrokinetic energy systems, catering to the unpredictable nature of aquatic environments.

Increasing the average power output through the DCCS not only enhances performance but also plays a crucial role in reducing the levelized cost of energy (LCOE). By optimizing the energy extraction efficiency, the DCCS ensures a higher average power production, which directly contributes to lowering the LCOE. This economic advantage, achieved by improved operational efficiency, fosters the competitiveness of hydrokinetic energy in the renewable market and supports the financial feasibility of sustainable energy projects.

The broader impact of this research is profound, extending beyond technological innovation to influence the future trajectory of renewable energy development. The DCCS elevates hydrokinetic energy to a new level of economic viability and environmental sustainability, positioning it as a competitive alternative to conventional energy sources. The ability of the DCCS to optimize energy extraction dynamically paves the way for a reevaluation of energy policies and investment strategies, potentially catalyzing a shift in the global energy market towards more sustainable and adaptable renewable energy solutions.

Furthermore, the success of DCCS in improving turbine performance and efficiency, along with reducing LCOE, promotes a rethinking of optimization strategies in the renewable energy sector. It calls for a more fluid, responsive approach to turbine control, encouraging the development of integrated systems that can adapt to environmental changes in real-time. This paradigm shift underscores the necessity for interdisciplinary collaboration in tackling the complexities of energy sustainability, advocating for a united effort among engineers,

environmental scientists, and economists to advance the renewable energy frontier.

In conclusion, the duct contraction control strategy represents a monumental stride in hydrokinetic turbine technology, offering a robust, experimentally validated solution to the challenges of dynamic water flow conditions. Its development not only epitomizes innovation in renewable energy technology but also heralds a new era of sustainable, efficient, and adaptable energy generation systems, with a significant impact on the economic landscape of renewable energy through the reduction of the levelized cost of energy.

5.2 Future Work

Exploring the DCCS sets the foundation, but it also paves the way for a range of prospective research directions aimed at enhancing the operational optimization of ducted HAHkT. A pivotal focus for subsequent studies is the integration of generator control mechanisms within the DCCS framework, an endeavor that stands to significantly elevate the system's adaptability and efficiency. Such advances would permit the dynamic alignment of power extraction with ever-changing flow conditions, optimizing energy harnessing while mitigating turbine wear and tear.

Furthermore, to date, investigations have predominantly been restricted to scenarios marked by lower-speed conditions and smaller duct configurations. Future research efforts must transcend these boundaries, delving into the implications of higher-speed conditions and larger duct configurations. This expansion is crucial for validating the DCCS's efficacy across a wider spectrum of flow velocities and turbine dimensions, thereby furnishing valuable insights into the system's scalability and its viability for deployment in natural water bodies.

Addressing the scalability of the research findings necessitates a meticulous evaluation of the nuanced challenges introduced by higher Reynolds numbers, potential modifications in flow characteristics, and the integrity of enlarged duct systems. Additionally, the real-world application of the DCCS requires an innovative adaptive duct design, a comprehensive assessment of environmental impacts, regulatory adherence, and economic feasibility to ensure

the sustainability and acceptance of the technology in various communities. Through dedicated exploration and innovation, future research efforts are poised to further the initial successes of this study, inching closer to the realization of the deployment of efficient, scalable and environmentally harmonious hydrokinetic energy systems, thus markedly contributing to the diversification and sustainability of global energy resources [6, 24, 28].

References

[1] Olabi, A. G. and Abdelkareem, Mohammad A. "Renewable energy and climate change." *Renewable and Sustainable Energy Reviews* Vol. 158 (2022): p. 112111. DOI 10.1016/j.rser.2022.112111.

[2] Neha and Joon, Rambeer. "Renewable energy sources: A review." *Journal of Physics: Conference Series* Vol. 1979 (2021): p. 012023. DOI 10.1088/1742-6596/1979/1/012023.

[3] Soeder, Daniel J. *A scientific assessment of the environmental risks from hydraulic fracturing and fossil fuels*. Springer (2021): pp. 155–185. DOI 10.1007/978-3-030-59121-2.

[4] Khan, M. J., Bhuyan, G., Iqbal, M. T. and Quaicoe, J. E. "Hydrokinetic energy conversion systems and assessment of horizontal and vertical axis turbines for river and tidal applications: A technology status review." *Applied Energy* Vol. 86 No. 10 (2009): pp. 1823–1835. DOI 10.1016/j.apenergy.2009.02.017.

[5] Laws, Nicholas D. and Epps, Brenden P. "Hydrokinetic energy conversion: Technology, research, and outlook." *Renewable and Sustainable Energy Reviews* Vol. 57 (2016): pp. 1245–1259. DOI 10.1016/j.rser.2015.12.189.

[6] Niebuhr, C. M., van Dijk, M., Neary, V. S. and Bhagwan, J. N. "A review of hydrokinetic turbines and enhancement techniques for canal installations: Technology, applicability and potential." *Renewable and Sustainable Energy Reviews* Vol. 113 (2019): p. 109240. DOI 10.1016/j.rser.2019.06.047.

[7] Chiang, Hsiao-Wei D., Lin, Chen-Yin and Hsu, Chih-Neng. "Design and performance study of an ocean current turbine generator." *International Journal of Turbo & Jet-Engines* Vol. 30 No. 3 (2013): pp. 293–302. DOI 10.1515/tjj-2013-0010.

[8] Luquet, R., Bellevre, D., Frechou, D., Perdon, P. and Guinard, P. "Design and model testing of an optimized ducted marine current turbine." *International Journal of Marine Energy* Vol. 2 (2013): pp. 61–80. DOI 10.1016/j.ijome.2013.05.009.

[9] Allsopa, Steven, Peyrard, Christophe, Thiesd, Philipp R., Boulougourise, Evangelos and Harrison, Gareth P. "Hydrodynamic analysis of a ducted, open centre tidal stream turbine using blade element momentum theory." *Ocean Engineering* Vol. 141 (2017): pp. 531–542. DOI 10.1016/j.oceaneng.2017.06.040.

[10] Boretti, Alberto. "State-of-the-art of MW-level capacity oceanic current turbines." *Nonlinear Engineering* Vol. 9 No. 1 (2020): pp. 361–369. DOI 10.1515/nleng-2020-0022.

[11] Kolekar, Nitin and Banerjee, Arindam. "A coupled hydro-structural design optimization for hydrokinetic turbines." *Journal of Renewable and Sustainable Energy* Vol. 5 No. 5 (2013): p. 053146. DOI 10.1063/1.4826882.

[12] Bilgen, Onur, Wang, Roger, Cao, Yue, Erol, Nazim and Shan, Xin. "A reconfigurable ducted turbine array concept for renewable flow energy harvesting." *AIAA SCITECH 2022 Forum*. AIAA 2022-2222: pp. 1–17. 2022. AIAA, San Diego, CA. DOI 10.2514/6.2022-2222.

[13] Góralczyk, Adam and Adamkowski, Adam. "Model of a Ducted Axial-Flow Hydrokinetic Turbine - Results of Experimental and Numerical Examination." *Polish Maritime Research* Vol. 25 (2018): pp. 113–122. DOI 10.2478/pomr-2018-0102.

[14] Ibrahim, Wan, Mohamed, M.R., Ismail, R.M.T.R., Leung, P.K., Xing, Wei and Shah, Akeel. "Hydrokinetic energy harnessing technologies: A review." *Energy Reports* Vol. 7 (2021): pp. 2021–2042. DOI 10.1016/j.egyr.2021.04.003.

[15] JENKS2026. "History of Wave and Tidal Energy." Green.org (2024). Accessed March 13, 2024, URL https://green.org/2024/01/30/history-of-wave-and-tidal-energy/.

[16] Sood, Manoj and Singal, Sunil K. "Development of hydrokinetic energy technology: A review." *International Journal of Energy Research* Vol. 43 No. 11 (2019): pp. 5552–5571. DOI 10.1002/er.4529.

[17] Khan, M Jahangir, Iqbal, M Tariq and Quaicoe, John E. "A technology review and simulation based performance analysis of river current turbine systems." *2006 Canadian Conference on Electrical and Computer Engineering*: pp. 2288–2293. 2006. IEEE. DOI 10.1109/CCECE.2006.277821.

[18] Sirois, Denis M. "Telesystem énergie." (2019). Accessed March 13, 2024, URL https://telesystemenergy.com/.

[19] Alipour, Ramin, Alipour, Roozbeh, Fardian, Farhad and Hossein Tahan, Mohammad. "Optimum performance of a horizontal axis tidal current turbine: A numerical parametric study and experimental validation." *Energy Conversion and Management* Vol. 258 (2022): p. 115533. DOI 10.1016/j.enconman.2022.115533.

[20] Wang, Jifeng and Müller, Norbert. "Performance prediction of array arrangement on ducted composite material marine current turbines (CMMCTs)." *Ocean engineering* Vol. 41 (2012): pp. 21–26. DOI 10.1016/j.oceaneng.2011.12.023.

[21] Li, Gang and Zhu, Weidong. "Tidal current energy harvesting technologies: A review of current status and life cycle assessment." *Renewable and Sustainable Energy Reviews*, Vol. 179: p. 113269. 2023. San Diego, CA. DOI 10.1016/j.rser.2023.113269.

[22] Jensen, Fergus and Asmarini, Wilda. "Tidal Power Developers Bet on Sea Change in Indonesia Renewables Sector." gCaptain (2016). Accessed March 14, 2024, URL https://gcaptain.com/tidal-power-developers-bet-sea-change-indonesia-renewables-sector/.

[23] Daglis, Daniel. "CRADA between Carderock, Oceana Energy Brings In-Stream Hydrokinetic Device to Marketplace." NSWC Carderock Division Public Affairs (2017). Accessed March 14, 2024, URL https://www.navsea.navy.mil/Media/News/Article/1109728/crada-between-carderock-oceana-energy-brings-in-stream-hydrokinetic-device-to-m/.

[24] Yuce, M. Ishak and Muratoglu, Abdullah. "Hydrokinetic energy conversion systems: A technology status review." *Renewable and Sustainable Energy Reviews* Vol. 43 (2015): pp. 72–82. DOI 10.1016/j.rser.2014.10.037.

[25] Masukume, Peace-Maker, Makaka, Golden and Tinarwo, David. "Technoeconomic Analysis of Ducted Wind Turbines and Their Slow Acceptance on the Market." *Journal of Renewable Energy* Vol. 2014 No. 951379 (2014): p. 5. DOI 10.1155/2014/951379.

[26] Zhou, Zhibin, Benbouzid, Mohamed, Charpentier, Jean-Frédéric, Scuiller, Franck and Tang, Tianhao. "Developments in large marine current turbine technologies – A review." *Renewable and Sustainable Energy Reviews* Vol. 71 (2017): pp. 852–858. DOI 10.1016/j.rser.2016.12.113.

[27] Finnegan, William, Jiang, Y., Meier, P., Hung, L. C., Fagan, E., Wallace, F., Glennon, C., Flanagan, M., Flanagan, T. and Goggins, J. "Numerical modelling, manufacture and structural testing of a full-scale 1 MW tidal turbine blade." *Ocean Engineering* Vol. 266 (2022): p. 112717. DOI 10.1016/j.oceaneng.2022.112717.

[28] Knight, Bradford, Freda, Robert, Young, Yin and Maki, Kevin. "Coupling Numerical Methods and Analytical Models for Ducted Turbines to Evaluate Designs." *Journal of Marine Science and Engineering* Vol. 6 No. 2 (2018): p. 43. DOI 10.3390/jmse6020043.

[29] Nigam, Suyash, Bansal, Shubham, Nema, Tanmay, Sharma, Vansh and Singh, Raj Kumar. "Design and pitch angle optimisation of horizontal axis hydrokinetic turbine with constant tip speed ratio." *MATEC Web of Conferences* Vol. 95 (2017): p. 06004. DOI 10.1051/matecconf/20179506004.

[30] Cui, Tonghui, Allison, James T. and Pingfeng, Wang. "Reliability-based control co-design of horizontal axis wind turbines." *Journal of Marine Science and Engineering* Vol. 64 No. 6 (2021): pp. 3653–3679. DOI 10.1007/s00158-021-03046-3.

[31] Fathy, Hosam K, Papalambros, Panos Y, Ulsoy, A Galip and Hrovat, Davor. "Nested plant/controller optimization with application to combined passive/active automotive suspensions." *Proceedings of the 2003 American Control Conference, 2003.*, Vol. 4: pp. 3375–3380. 2003. IEEE. DOI 10.1109/ACC.2003.1244053.

[32] Namik, H. and Stol, K. "Individual blade pitch control of floating offshore wind turbines." *Wind Energy* Vol. 13 No. 1 (2010): pp. 74–85. DOI 10.1002/we.332.

[33] Posa, A. and Broglia, R. "Energy From The Oceans: Simulations Help To Design Efficient Tidal Turbine Farm." Partnership for Advanced Computing in Europe (2021). Accessed

March 13, 2024, URL https://prace-ri.eu/energy-from-the-oceans-high-fidelity-simulations-help-to-design-efficient-tidal-turbine-farms/.

[34] Shinomiya, L. D., Vaz, J. R. P., Mesquita, A. L. A., de Oliveira, T. F., Brasil Junior, A. C. P. and Silva, P. A. S. F. "An approach for the optimum hydrodynamic design of hydrokinetic turbine blades." *Revista de Engenharia Térmica* Vol. 14 No. 2 (2015): pp. 43–46. DOI 10.5380/reterm.v14i2.62131.

[35] Pournazeri, S., Aghsaee, P., Mantilla, R. and Markfort, C. "Optimization and initial testing of a model-scale horizontal axis hydrokinetic turbine." *The International Conference On Fluvial Hydraulics (River Flow 2016)*: pp. 2148–2153. St. Louis, MO, June 6, 2016. DOI 10.1201/9781315644479-334.

[36] Phan, Thanh-Hoang, Kadivar, Ebrahim, Nguyen, Van-Tu, el Moctar, Ould and Park, Warn-Gyu. "Thermodynamic effects on single cavitation bubble dynamics under various ambient temperature conditions." *Physics of Fluids* Vol. 34 No. 2 (2022): p. 023318. DOI 10.1063/5.0076913.

[37] Muratoglu, Abdullah and Yuce, Mehmet. "Performance analysis of hydrokinetic turbine blade sections." *Advances in Renewable Energy* Vol. 2 (2015): pp. 1–10.

[38] Chudzik, Stanislaw. "Wind Microturbine with Adjustable Blade Pitch Angle." *Energies* Vol. 16 (2023): p. 945. DOI 10.3390/en16020945.

[39] Yunus, A. Cengel. *Fluid Mechanics: Fundamentals And Applications (SI Units)*. Tata McGraw Hill Education Private Limited (2010).

[40] Elkolali, Moustafa, Splawski, Wilfried A., Carella, Alfredo and Alcocer, Alex. "Hydrodynamic parameter optimization for miniature underwater glider wings." *Global Oceans 2020: Singapore – U.S. Gulf Coast*: pp. 1–8. Singapore, October 5–30, 2020. IEEE. DOI 10.1109/IEEECONF38699.2020.9389187.

[41] Kulunk, Emrah. "Aerodynamics of Wind Turbines." *Fundamental and Advanced Topics in Wind Power*. IntechOpen, Rijeka, Croatia (2011), Chap. 1. DOI 10.5772/17854.

[42] Somers, D. M. "S833, S834, and S835 Airfoils: November 2001–November 2002." Technical Report No. NREL/SR-500-36340. National Renewable Energy Lab, Golden, CO. 2005. DOI 10.2172/15020040.

[43] Laín, Santiago, Contreras, Leidy T. and López, Omar D. "A review on computational fluid dynamics modeling and simulation of horizontal axis hydrokinetic turbines." *Journal of the Brazilian Society of Mechanical Sciences and Engineering* Vol. 41 No. 9 (2019): p. 375. DOI 10.1007/s40430-019-1877-6.

[44] Chang, Ling-Yuan, Chen, Falin and Tseng, Kuo-Tung. "Dynamics of a Marine Turbine for Deep Ocean Currents." *Journal of Marine Science and Engineering* Vol. 4 No. 3 (2016): p. 59. DOI 10.3390/jmse4030059.

[45] Lawn, C. J. "Optimization of the power output from ducted turbines." *Journal of Power and Energy* Vol. 217 No. 1 (2003): pp. 107–117. DOI 10.1243/095765003321148754.

[46] Knowlton, T. M. *10 - Fluidized bed reactor design and scale-up*. Woodhead Publishing Series in Energy, Woodhead Publishing (2013). DOI 10.1533/9780857098801.2.481.

[47] Doman, Darrel A., Murray, Robynne E., Pegg, Michael J., Gracie, Katie, Johnstone, Cameron M. and Nevalainen, Thomas. "Tow-tank testing of a 1/20th scale horizontal axis tidal turbine with uncertainty analysis." *International Journal of Marine Energy* Vol. 11 (2015): pp. 105–119. DOI 10.1016/j.ijome.2015.06.003.

[48] Güney, M.S. and Kaygusuz, K. "Hydrokinetic energy conversion systems: A technology status review." *Renewable and Sustainable Energy Reviews* Vol. 14 No. 9 (2010): pp. 2996–3004. DOI 10.1016/j.rser.2010.06.016.

[49] Käse, Laura and Geuer, Jana K. *Phytoplankton Responses to Marine Climate Change - An Introduction: Proceedings of the 2017 conference for YOUng MARine RESearchers in Kiel, Germany*. Springer International Publishing (2018): pp. 55–71. DOI 10.1007/978-3-319-93284-2_5.

[50] Bahaj, A. S. and Myers, L. E. "Fundamentals applicable to the utilisation of marine current turbines for energy production." *Renewable Energy* Vol. 28 No. 14 (2003): pp. 2205–2211. DOI 10.1016/S0960-1481(03)00103-4.

[51] Hodgkin, Amy, Laizet, Sylvain and Deskos, Georgios. "Numerical investigation of the influence of shear and thermal stratification on the wind turbine tip-vortex stability." *Wind Energy* Vol. 25 No. 7 (2022): pp. 1270–1289. DOI 10.1002/we.2728.

[52] Alaskari, Mustafa, Abdullah, Oday and Majeed, Mahir H. "Analysis of wind turbine using QBlade software." *IOP Conference Series: Materials Science and Engineering* Vol. 518 No. 3 (2019): p. 032020. DOI 10.1088/1757-899X/518/3/032020.

[53] Marten, David, Peukert, Juliane, Pechlivanoglou, Georgios, Nayeri, Christian and Paschereit, Christian. "QBLADE: An open source tool for design and simulation of horizontal and vertical axis wind turbines." *International Journal of Emerging Technology and Advanced Engineering* Vol. 3 No. 3 (2013): pp. 264–269.

[54] Batten, W. M. J., Bahaj, A. S., Molland, A. F. and Chaplin, J. R. "Experimentally validated numerical method for the hydrodynamic design of horizontal axis tidal turbines." *Ocean Engineering* Vol. 34 No. 7 (2007): pp. 1013–1020. DOI 10.1016/j.oceaneng.2006.04.008.

[55] Drela, M. "XFOIL: An Analysis and Design System for Low Reynolds Number Airfoils." *Low Reynolds Number Aerodynamics*: pp. 1–12. Berlin, Heidelberg, 1989. IEEE. DOI 10.1007/978-3-642-84010-4_1.

[56] van Kuik, G. A. M. *The actuator disc concept*. Springer (2020): pp. 1–49. DOI 10.1007/978-3-030-05455-7_2-2.

[57] Naderi, Shayan and Torabi, Farschad. "Numerical investigation of wake behind a HAWT using modified actuator disc method." *Energy Conversion and Management* Vol. 148 (2017): pp. 1346–1357. DOI 10.1016/j.enconman.2017.07.003.

[58] Branlard, Emmanuel. *Wind Turbine Aerodynamics and Vorticity-Based Methods*, 1st ed. Vol. 7 of *Research Topics in Wind Energy*. Springer International Publishing AG, Cham (2017). DOI 10.1007/978-3-319-55164-7.

[59] Ragheb, Magdi and Ragheb, Adam M. *Wind Turbines Theory - The Betz Equation and Optimal Rotor Tip Speed Ratio, Fundamental and Advanced Topics in Wind Power*. Intech, Rijeka, Croatia (2011). DOI 10.5772/21398.

[60] Betz, Albert. "The maximum of the theoretically possible utilization of the wind by wind motors." *Magazine for the entire turbine West* Vol. 20 (1920).

[61] Ingram, Grant. *Wind turbine blade analysis using the blade element momentum method. version 1.1*. Durham University (2011).

[62] Bangga, Galih. "Comparison of Blade Element Method and CFD Simulations of a 10 MW Wind Turbine." *Fluids* Vol. 3 No. 4 (2018): p. 73. DOI 10.3390/fluids3040073.

[63] van den Broek, Sander. "Towards High-Fidelity Aeroelastic Analysis of Wind Turbines." Ph.D. Thesis, Delft University of Technology. 2013. DOI 10.13140/RG.2.2.19745.97121.

[64] Gauert, H. *Aerodynamic Theory*. Springer Berlin Heidelberg, Berlin (1935): pp. 169–360. DOI 10.1007/978-3-642-91487-4_3.

[65] da Silva, Paulo Augusto Strobel Freitas, Shinomiya, Léo Daiki, de Oliveira, Taygoara Felamingo, Vaz, Jerson Rogério Pinheiro, Mesquita, André Luiz Amarante and Junior, Antonio Cesar Pinho Brasil. "Design of hydrokinetic turbine blades considering cavitation." *Energy Procedia* Vol. 75 (2015): pp. 277–282. DOI 10.1016/j.egypro.2015.07.343.

[66] Brahimi, Tayeb and Paraschivoiu, Ion. *Aerodynamic Analysis and Performance Prediction of VAWT and HAWT Using CARDAAV and Qblade Computer Codes*. IntechOpen (2021): pp. 326–456. DOI 10.5772/intechopen.96343.

[67] Contreras, Leidy Tatiana, Lopez, Omar Dario and Lain, Santiago. "Computational fluid dynamics modelling and simulation of an inclined horizontal axis hydrokinetic turbine." *Energies* Vol. 11 No. 11 (2018): p. 3151. DOI 10.3390/en11113151.

[68] Masters, Ian, Chapman, JC, Willis, MR and Orme, JAC. "A robust blade element momentum theory model for tidal stream turbines including tip and hub loss corrections." *Journal of Marine Engineering and Technology* Vol. 10 No. 1 (2011): pp. 25–35. DOI 10.1080/20464177.2011.11020241.

[69] Noruzi, R., Vahidzadeh, M. and Riasi, A. "Design, analysis and predicting hydrokinetic performance of a horizontal marine current axial turbine by consideration of turbine installation depth." *Ocean Engineering* Vol. 108 (2015): pp. 789–798. DOI 10.1016/j.oceaneng.2015.08.056.

[70] Shahsavarifard, Mohammad, Bibeau, Eric L. and Birjandi, Amir Hossein. "Performance gain of a horizontal axis hydrokinetic turbine using shroud." *OCEANS 2013 - San Diego*: pp. 1–5. San Diego, CA, Septemeber 23–27, 2013. IEEE. DOI 10.23919/OCEANS.2013.6740968.

[71] Barbarić, M. and Guzović, Z. "Investigation of the Possibilities to Improve Hydrodynamic Performances of Micro-Hydrokinetic Turbines." *Energies* Vol. 13 No. 17 (2020): p. 4560. DOI 10.3390/en13174560.

[72] Bahaj, A.S., Molland, A.F., Chaplin, J.R. and Batten, W.M.J. "Power and thrust measurements of marine current turbines under various hydrodynamic flow conditions in a cavitation tunnel and a towing tank." *Renewable Energy* Vol. 32 No. 3 (2007): pp. 407–426. DOI 10.1016/j.renene.2006.01.012.

[73] Vaz, Déborah A. T. D. do Rio, Vaz, Jerson R. P. and Silva, Paulo A. S. F. "An approach for the optimization of diffuser-augmented hydrokinetic blades free of cavitation." *Energy for Sustainable Development* Vol. 45 (2018): pp. 142–149. DOI 10.1016/j.esd.2018.06.002.

[74] An, Yongkai, Lu, Wenxi and Cheng, Weiguo. "Surrogate model application to the identification of optimal groundwater exploitation scheme based on regression kriging method-a case study of Western Jilin Province." *International journal of environmental research and public health* Vol. 12 No. 8 (2015): pp. 8897–8918. DOI 10.3390/ijerph120808897.

[75] Tapoglou, Evdokia, Karatzas, George P, Trichakis, Ioannis C and Varouchakis, Emmanouil A. "A spatio-temporal hybrid neural network-Kriging model for groundwater level simulation." *Journal of hydrology* Vol. 519 (2014): pp. 3193–3203. DOI 10.1016/j.jhydrol.2014.10.040.

[76] Modis, K and Sideri, D. "Spatiotemporal estimation of land subsidence and ground water level decline in West Thessaly basin, Greece." *Natural Hazards* Vol. 76 (2015): pp. 939–954. DOI 10.1007/s11069-014-1528-2.

[77] Kwon, Hyungil, Yi, Seulgi and Choi, Seongim. "Numerical investigation for erratic behavior of Kriging surrogate model." *Journal of Mechanical Science and Technology* Vol. 28 (2014): pp. 3697–3707. DOI 10.1007/s12206-014-0831-x.

[78] Xia, Bin, Ren, Ziyan and Koh, Chang-Seop. "Utilizing kriging surrogate models for multi-objective robust optimization of electromagnetic devices." *IEEE transactions on magnetics* Vol. 50 No. 2 (2014): pp. 693–696. DOI 10.1109/TMAG.2013.2284925.

[79] Bilicz, Sándor, Lambert, Marc, Gyimothy, Szabolcs and Pavo, Jozsef. "Solution of inverse problems in nondestructive testing by a kriging-based surrogate model." *IEEE Transactions on Magnetics* Vol. 48 No. 2 (2012): pp. 495–498. DOI 10.1109/TMAG.2011.2172196.

[80] Toal, J., David, J. and Keane, Andy J. "Performance of an ensemble of ordinary, universal, non-stationary and limit Kriging predictors." *Structural and Multidisciplinary Optimization* Vol. 47 (2013): pp. 893–903. DOI 10.1007/s00158-012-0866-5.

[81] Horowitz, Bernardo, Afonso, Silvana Maria Bastos and de Mendonça, Carlos Victor Paiva. "Surrogate based optimal waterflooding management." *Journal of Petroleum Science and Engineering* Vol. 112 (2013): pp. 206–219. DOI 10.1016/j.petrol.2013.11.006.

[82] Hew, W. R., Saat, F. A. Z. Mohd, Irfan, A. R., Mattokit, E., Rosli, M. A. M., Anuar, F. Shikh, Herawan, S. G. and Syahputra, S. I. A. "Computational fluid dynamics modelling of a hydrokinetic turbine." *AIP Conference Proceedings* Vol. 2347 No. 1 (2021): p. 020195. DOI 10.1063/5.0051477.

[83] Bayat, Saeid, Lee, Yong Hoon and Allison, James T. "Control co-design of horizontal floating offshore wind turbines using a simplified low order model." *Wind Energy Science Conference*: pp. 1–3. Hannover, Germany, May 25–28, 2021.

[84] Gray, Justin S., Hwang, John T., Martins, Joaquim R. R. A., Moore, Kenneth T. and Naylor, Bret A. "OpenMDAO: An Open-Source Framework for Multidisciplinary Design, Analysis, and Optimization." *Structural and Multidisciplinary Optimization* Vol. 59 No. 4 (2019): pp. 1075–1104. DOI 10.1007/s00158-019-02211-z.

[85] Andres, M. "Spatial and Temporal Variability of the Gulf Stream Near Cape Hatteras." *Journal of Geophysical Research: Oceans* Vol. 126 No. 9 (2021): p. e2021JC017579. DOI 10.1029/2021JC017579.

[86] Hasan, Mehedi, El-Shahat, Adel and Rahman, Mosfequr. "Performance investigation of three combined airfoils bladed small scale horizontal axis wind turbine by BEM and CFD analysis." *Journal of Power and Energy Engineering* Vol. 5 No. 5 (2017): pp. 14–27. DOI 10.4236/jpee.2017.55002.